

# MEDITERRANEAN OUTFLOW: ACROSS THE GLACIAL TERMINATION

The meltdown of the Greenland ice cap could reduce the formation of deep water in the North Atlantic thereby slowing down the Atlantic Meridional Overturning Circulation (AMOC). A reduced overturning might subsequently affect the climate of Western Europe. On glacial to interglacial timescales strengthened MOW provided a negative feedback to North Atlantic freshening boosts quickly rebooting a reduced or inactive AMOC. The last glacial to interglacial transition has witnessed several rapid transitions in overturning induced by these changes in the northern salinity budget. This study therefore aimed to reconstruct the density (and strength) of the MOW across the last termination. Trace elemental and clumped isotope temperatures extracted from benthic foraminifera preserved in deep sea sediments in the Gulf of Cadiz provided a high resolution salinity record of the lower core of MOW over the last 21,000 years. Although bottom water salinity was higher in the LGM the lower core reduced in density across the cold H1 and YD stadials. Furthermore stagnation of the water column during the deposition of S1 resulted in a complete shutdown of the lower core of MOW. The deeper branch of Mediterranean Outflow is thus concluded to be incapable of sustaining overturning across the last termination. Additional research should nevertheless aim on reconstructing both the lower and the upper core of outflow. The upper core might turn out to be more influential. An accurate reconstruction of the MOW its flow path and insights into the influence of the Iberian delta on the regional hydrography can resolve several uncertainties. Improvements of the Mg/Ca and clumped isotope thermometry are required in order to further increase the accuracy of the bottom water temperature reconstructions. Moreover, epifaunal benthics supplied the most accurate temperature reconstructions.

*Master Thesis*

*Joep van Dijk*

*Supervisors:*

*Martin Ziegler  
(UU)*

*Lucas Lourens  
(UU)*

*Thanks:*

*Lennart de  
Nooijer (NIOZ)  
and Wim Boer  
(NIOZ)*

## Table of Contents

1.	Climate change and the AMOC .....	3
1.1.	Dynamics and consequences of changing AMOC.....	3
1.2.	Climate transitions in the past: different states of AMOC .....	5
1.2.1.	The Late Quaternary climate: glacials and interglacials.....	6
1.2.2.	Secondary climate oscillations: Heinrich and Dansgaard-Oeschger events .....	7
1.2.3.	The last glacial to interglacial transition: the role of the carbon cycle .....	9
2.	Filling in the gaps: The Mediterranean Outflow .....	10
3.	Methodology .....	12
3.1.	Strategies and studied site .....	12
3.2.	Applied proxies .....	13
3.2.1.	Stable isotopes .....	13
3.2.2.	Mg/Ca paleothermometry .....	14
3.2.3.	Clumped paleothermometry .....	15
3.2.4.	Grain size and magnetic susceptibility .....	16
3.3.	Sampling and proxy recovery .....	16
3.4.	Bottom water salinity estimation .....	17
3.5.	Age model.....	18
4.	Modern hydrography .....	19
5.	Results .....	21
5.1.	Stable isotopes .....	21
5.2.	Bottom water temperature and salinity .....	23
6.	Discussion .....	24
6.1.	Problems involving the temperature reconstructions.....	25
6.1.1.	Cleaning protocol.....	25
6.1.2.	Calibrations .....	26
6.2.3	Applicability of the clumped paleothermometer .....	28
6.2.	Evolution of Mediterranean Outflow .....	29
6.2.1.	Across the termination .....	29
6.2.2.	H1, AB and the YD.....	30
6.2.3.	S1 .....	31
6.3.	Evaluation of the shallow source hypothesis .....	32
6.4.	Outlook.....	33
7.	Conclusion .....	34
	Appendices.....	35
	References .....	37

# 1. Climate change and the AMOC

In May this year atmospheric CO<sub>2</sub> reached concentrations of over 400 ppm [NASA]. Although this is just a meaningless number to many, to some it proves the extent to which mankind can force atmospheric and consequential climatic change. Earth's climate is warming and the most recent IPCC report states that the cause of this warming is extremely unlikely to be the result of natural processes alone. One of the main impacts of this warming is the rapid meltdown of ice stored on and around Greenland. The subsequent sea level rise is already known to affect the coastal habitability in Europe. It is predicted that by the year 2300 the sea level in the North Sea will have risen by 50-200 cm [Slangen et al., 2012]. Furthermore, state-of-the-art climate models project a gradual decline of the strength of the Atlantic Meridional Overturning Circulation (AMOC) [IPCC AR5, 2013]. The AMOC is a key component of Earth's climate [see section 1.1].

The aim of this study is to infer to what extent the Mediterranean Outflow sustained or even promoted the strength of the AMOC across the last glacial to interglacial transition. The Mediterranean Outflow is a relatively dense water mass that enters the North Atlantic Ocean through the strait of Gibraltar (Fig. 1). In order to emphasize the importance of this water mass in relation to the AMOC, some background information is required. In the next section of this chapter, the dynamics of Atlantic overturning are briefly introduced. Furthermore, both the cause for and the consequences of a reduced AMOC are clarified. In section 1.2 AMOC dynamics in relation to past climate transitions are introduced. The aims of this study are introduced in chapter 2.

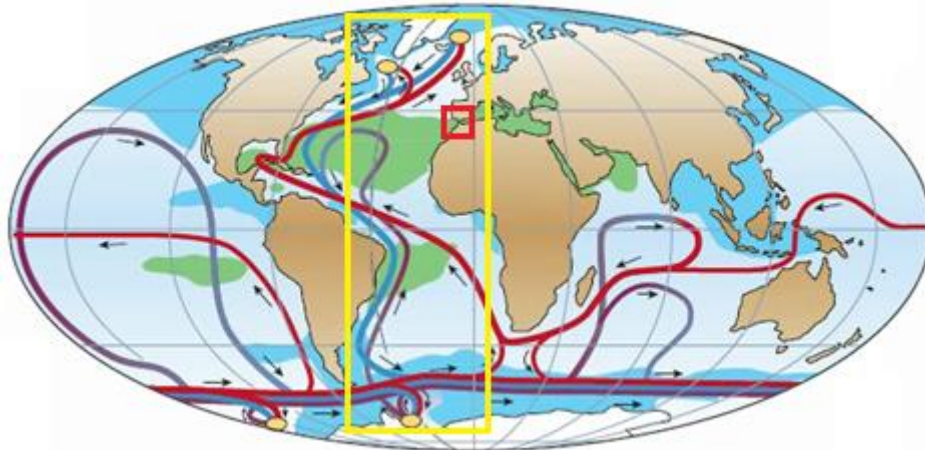


Figure 1: Simplified sketch of global ocean circulation (zone of AMOC highlighted in yellow). Near-surface waters (red) flow towards four main deep-water formation regions (yellow ovals; the Labrador and Greenland-Iceland-Norwegian (GIN) Seas in the North Atlantic and the Weddell and Ross Seas in the Southern Ocean) and recirculate at depth (deep currents shown in blue, bottom currents in purple). Especially in the Southern Ocean deep water is returned to the surface. Green shading indicates salinity above 36‰, blue shading indicates salinity below 34‰. The location at which the Mediterranean Outflow enters the Atlantic Ocean is highlighted in red [adapted from Rahmstorf, 2002].

## 1.1. Dynamics and consequences of changing AMOC

The AMOC can be subdivided in five oceanographic subdivisions which act within the oceanic part of the yellow grid box in Figure 1. First, trade winds drive a regular current system in the upper layers of the ocean, forced by the sun and spinning of the Earth, which sustains a net transport of warm (red) waters to the north along with the Gulf Stream and the North Atlantic Current (NAC).

Second, warm water releases its accumulated heat in the North Atlantic and consequentially increases in density after which it sinks down. Descending water (blue) accumulates as North Atlantic

Deep Water (NADW) along the continental margins of the Labrador and GIN Seas in relation to deep convection [Marshall and Scott, 1999; Spall and Pickart, 2001].

Third, in the Southern Ocean, deep water is brought to the surface due to vigorous Ekman pumping induced by westerly winds [Döös and Coward, 1997; Rintoul et al., 2001; Gnanadesikan and Hallberg, 2002] and the Drake Passage Effect [Toggweiler and Samuels, 1995; Kuhlbrodt et al., 2007].

Fourth, in the Weddell and Ross Seas, the density of Antarctic Circumpolar Current (ACC) water becomes even higher than in the north when confronted with brine formation induced by Antarctic katabatic winds [Aagard, 1981]. This Antarctic Bottom Water (AABW) thus descends to larger depths than the NADW. Nevertheless, AABW (purple in Fig. 1) returns to the surface south of the equator as a result of diapycnal mixing [see Garrett and St. Laurent, 2002; Wunsch and Ferrari, 2004; Kuhlbrodt et al., 2007].

Fifth, the deep NADW current flows from the North Atlantic to the Southern Ocean forced by a horizontal pressure gradient. This gradient is driven by net upwelling in the Southern Ocean [Toggweiler and Samuels, 1993, 1995, 1998; Samelson, 2004]. A depth cross section of AMOC further emphasizes these five subdivisions (Figure 2).

The AMOC thus exerts a strong control on the stratification and distribution of water masses, the amount of heat that is transported, and subsequently the cycling and storage of chemical species such as carbon dioxide in the deep sea. Clearly, the AMOC is a key component of Earth's climate system.

Near-surface water freshening due to ice melt, to precipitation and mid-latitude warming is projected to reduce the strength of AMOC especially in relation to a decrease in the formation of NADW [IPCC AR5, 2013]. Ice melt, for example, can potentially increase the stratification in the North Atlantic Seas preventing deep convection [Kuhlbrodt et al., 2007]. A reduction in the strength of AMOC has several consequences which underline the importance of studying AMOC dynamics.

At present, the Gulf Stream and the NAC are responsible for about 1 PW of yearly heat transport to the North Atlantic [Hall and Bryden, 1982; Ganachaud and Wunsch, 2000; Trenberth and Caron, 2001]. This heat transport drives a predominant mild climate in northwestern Europe. A reduction in the strength of AMOC could reduce this comfort as shown in Figure 3 [Maslin et al., 2001; Winton, 2003]. Furthermore it could have strong implications for the El Niño-Southern Oscillation phenomenon [Timmermann et al., 2005] and the position of the Intertropical Convergence Zone [Vellinga and Wood, 2002]. Moreover it could lower the uptake of CO<sub>2</sub> by the deeper ocean due to an increased stratification in the North Atlantic [Maier-Reimer et al., 1996; Sarmiento and Le Quéré, 1996; Marchal et al., 1998; Matear and Hirst, 1999; Joos et al., 1999; Plattner et al., 2001; Ewen et al., 2004; Obata, 2007; Zickfeld et al., 2008] and a decrease in the biological pump [Maier-Reimer et al., 1996; Sarmiento and Le Quéré, 1996; Marchal et al., 1998; Joos et al., 1999; Plattner et al., 2001; Schmittner, 2005; Schmittner et al., 2007]. A reduced AMOC could in the end even have implications for the marine ecosystem in the North Atlantic [Schmittner, 2005].

Nevertheless, the trustworthiness of the modelled projections is in dispute due to the profound error margins. There are several reasons for these uncertainties.

First, the fundamental process behind deep water formation in the North Atlantic is not yet perfectly understood. This is partly due to the fact that oceanographic research in the North Atlantic is mostly limited to the summer season. Models a priori lack a perfect parameterization of the sinking branch of AMOC, although progress is being made [Straneo, 2008; Spall, 2010; Gelderloos et al., 2011; Våge et al., 2013]. Moreover, modelling studies in general suffer from errors induced by the coarse resolutions which hamper the accuracy of the physical simulations.

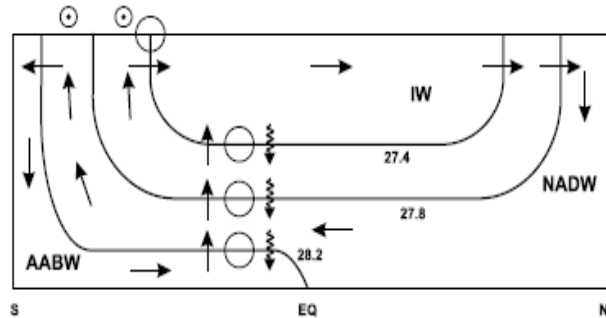


Figure 2: Meridional box model of the two cells of overturning (AABW and NADW) with light Intermediate Waters (IW) on top. Lines indicate isopycnal surfaces with respective densities. Dense-to-light conversion induced by diapycnal mixing occurs at the open circles. Wind-driven upwelling is indicated by dotted circles. NADW formation is mainly driven by buoyancy fluxes [Kuhlbrodt et al., 2007].

Another problem is the lack of an understanding of the sensitivity of AMOC under different boundary conditions. The dynamics of AMOC as summarized in section 1.1 are very simplified. Especially the relationship between the AMOC and the Northern ice sheet dynamics is determined by more than just the melting of ice. In fact together with the climate in the North Atlantic the three systems closely interact and intertwine, making it a complex system quite hard to comprehend when only deducing present observations.

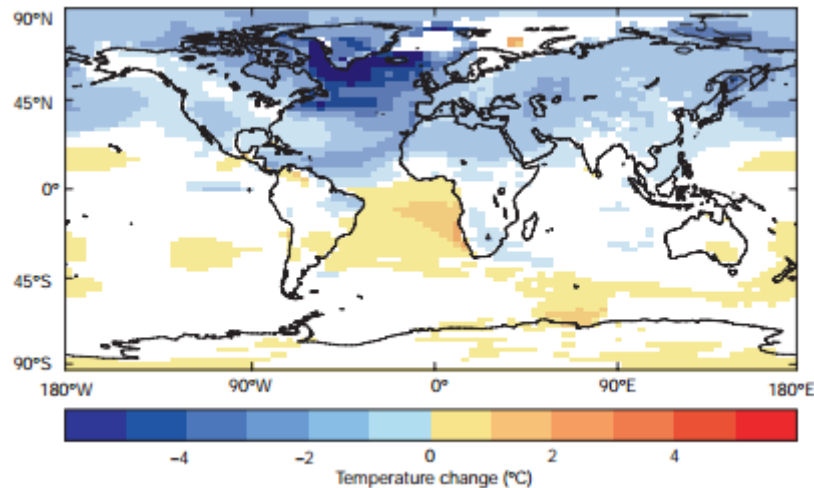


Figure 3: Changes in surface air temperature caused by a shutdown of NADW formation in a current ocean-atmosphere circulation model. Note the hemispheric see-saw (Northern Hemisphere cools while the Southern Hemisphere warms) and the maximum cooling over the northern Atlantic. Deep water formation sites are not realistically simulated due to the coarse resolution.

Another approach to gain a better understanding of the sensitivity of AMOC is by looking into the past; the geological archives. Through stratigraphic conversion of depth to age, these archives provide insights into past AMOC dynamics. Two fundamental geological archives are the deep marine sediment and the ice core record.

Deep marine sediments have accumulated over a range of millions of years and even older marine sediments have returned to the land induced by plate tectonics. Sediments contain endless fossils, organic substances and trace elements. These contents reflect specific quantities of the paleo-environment (e.g. temperature, salinity and oxygenation). Evidently, in order to reconstruct the paleo-environment one has to relate content to a specific quantity. By doing so, environmental proxies are established.

Apart from water vapour, the precipitation of ice on both the Northern and the Southern Hemisphere also takes up other gases (e.g.  $\text{CH}_4$  and  $\text{CO}_2$ ) from the atmosphere. Similar to the deep marine proxies, these gases can be used to reconstruct the atmosphere of the past.

Studies of both archives [Bond et al., 1992; Maslin et al., 2001; Clark et al., 2002; Rahmstorf, 2002; McManus et al., 2004] suggest that there have been completely different Atlantic circulation dynamics in the past. Furthermore, transitions between two relatively stable states of climate occurred within relatively short periods of time. The next section provides a detailed description of the past AMOC states in relation to these climate transitions.

## 1.2. Climate transitions in the past: different states of AMOC

In Figure 4 the most important climate transitions of the Quaternary Period have been summarized. The events highlighted in yellow have been fundamental for the climate as it is today. The transitions highlighted in red are most relevant for this study since global warming might result in similar transitions in the future (see section 1.2.2). In the next section events in climate from 10 Ma up to 100 ka, are briefly described.

### 1.2.1. The Late Quaternary climate: glacials and interglacials

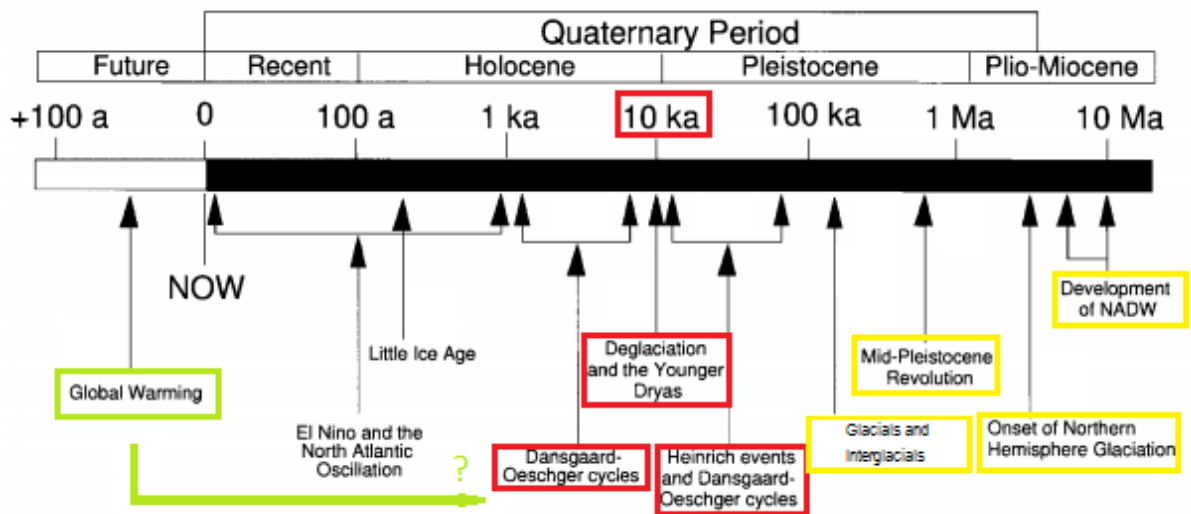


Figure 4: Climate events in the Quaternary Period. Will global warming induce rapid climate transitions as has happened in the past?

The AMOC as it is known today developed around 10 Myr ago with the initiation of NADW formation in response to the closure of the Panama gateway [Nisancioglu et al., 2003]. In relation to this closure, but especially due to a global cooling trend which started around 50 Ma, ice accumulation initiated on Greenland between 10 and 6 Ma [Jansen et al, 1990; Wolf and Thiede; 1991; Jansen and Sjolholm, 1991; Wolf-Welling et al, 1995]. A review by Maslin et al. in 2001 provides a summary of the processes that led to this global cooling trend.

Around 2.75 Ma northern ice sheets reached a substantial size [Raymo, 1994; Maslin, 1998] and started to interfere with the climate system. Changes in incoming solar radiation initiated phases of net ice growth and melt; glacials and interglacials or deglaciations. It is widely accepted that natural variability in the orbital parameters forced these changes in insolation [Milankovitch, 1949; Hays et al., 1976; 1984; Ruddiman and McIntyre, 1981; Imbrie et al, 1992; 1993; Berger and Loutre, 1991; Laskar, 1990]. Up around 1 Ma, a glacial to interglacial transition took place every 41 kyr, after which the transitions took place roughly every 100 kyr. This change in periodicity has been related to an increase in the stability of the northern ice sheets and is defined as the Mid-Pleistocene Revolution [see further Maslin et al., 2001].

It should be noted that although the Northern Hemispheric ice sheets have witnessed periods of both waxing and waning, the Antarctic ice sheet has remained relatively stable over the last 2.5 Myrs [Maslin et al., 2001, Ruddiman, 2008].

Thus, orbital forcing triggered the start of both a glacial and interglacial climate state. A sequence of internal feedback mechanisms is suggested to translate this external force into a global change in climate. The conventional view is that ice initially starts to build-up on the northern continents at times of cool northern summers [Milankovitch, 1949]. Next, the northern ice sheet produces its own sustainable environment primarily by increasing the albedo [e.g., Hewitt and Mitchell, 1997]. The third stage is when the ice sheets become big enough to deflect the atmospheric planetary waves [COHMAP, 1988]. This changes the storm path across the North Atlantic Ocean and prevents the warm and saline Gulf Stream to penetrate as far north as today. The subsequent decrease in northward surface currents prevents warm and saline water from entering the Nordic Seas which ultimately reduces the production of deep water [Broecker, 1991]. This in turn reduces the amount of water pulled northwards. All of which leads to an increased cooling of the Northern Hemisphere and further expansion of the ice sheets. The gradual build-up of ice is accurately recorded by proxy records within the Greenland ice sheet (see Fig. 5 in section 1.2.2).

Secondary feedback mechanisms induced by the carbon, methane [Sigman and Boyle, 2000] and water vapour [Lea et al., 2000] cycles, help drive the system towards the maximum possible

glacial conditions. Naturally as warm surface water is forced further and further south, supply of moisture that is required to build ice sheets decreases which prevents the feedback systems from becoming a 'run-away' effect [Maslin et al., 2001].

Due to the fact that ice sheets are naturally unstable [Dowdeswell et al., 1999] feedback mechanisms are constantly altering direction during the whole glacial period. This instability is likely responsible to the relatively rapid secondary oscillations within the glaciations [Maslin et al., 2001]; the Dansgaard Oeschger cycles and Heinrich events. The next section is addressed to these secondary climate oscillations.

### 1.2.2. Secondary climate oscillations: Heinrich and Dansgaard-Oeschger events

Two figures help to explain the Late Quaternary rapid climate transitions. Figure 5 shows the glacial to interglacial transitions over the last 1 Myrs. Note that  $\delta^{18}\text{O}$  is a proxy for ice volume with low values corresponding to relatively low ice volume on the poles [see section 3.2]. The dashed line is defined as the maximum stable ice volume on the Northern Hemisphere [see Denton et al., 2010]. Most terminations (T) take place after the build-up has reached this 'stability threshold'. Furthermore, most terminations occur in response to maxima in summer insolation on the Northern Hemisphere.

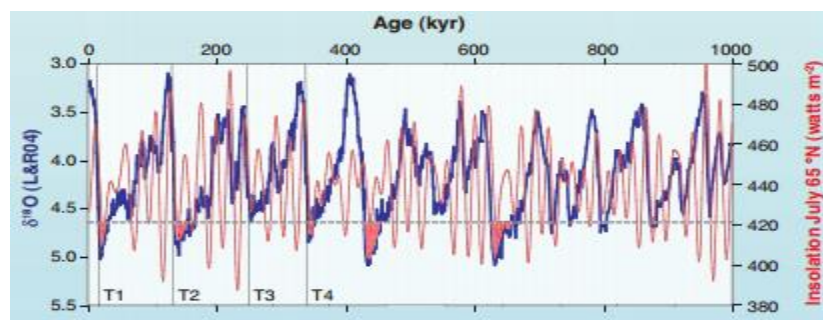


Figure 5: Glacial to interglacial transitions over the last 1 Ma constructed with the LR04 stack [Lisiecki and Raymo, 2004].  $\Delta^{18}\text{O}$  is negatively related to ice volume on the poles. The dashed-line represents the maximum stable volume of ice on the Northern Hemisphere. T1 to T4 stand for the last four glacial terminations [Adapted from Denton et al., 2010]. July insolation  $65^\circ\text{N}$  matches the general transitions [Laskar, 1990].

Figure 6 zooms in on the last glacial to interglacial transition. At first, it is observed that although the glaciation phase is relatively long, deglaciation occurs within roughly 4 kyr. Second, a series of Dansgaard-Oeschger (D-O) and Heinrich (H) events precede the transition towards the present interglacial climatic state. Third, H1 and the Younger Dryas (YD or H0) occur within a period of 4 kyr alternated with the warm Allerød/Bølling event (D-O 1). Last, the D-O cycles have the tendency to occur at intervals of 1,470 years or multiples thereof [Rahmstorf, 2002]

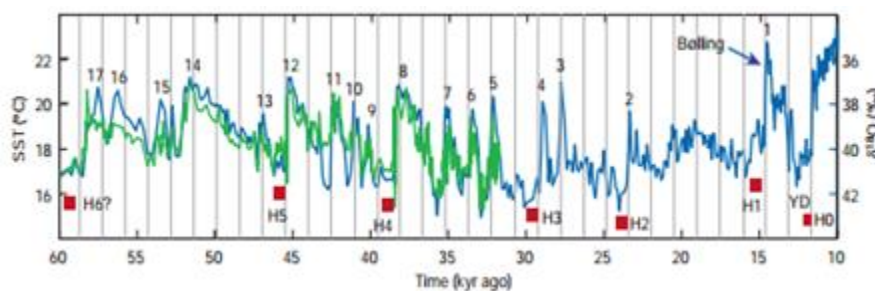


Figure 6: Temperature reconstructions from ocean sediments and Greenland ice. Proxy data from the subtropical Atlantic (green) [Sachs and Lehman, 1999] and from the Greenland ice core GISP2 (blue) [Groote et al., 1993] show several Dansgaard-Oeschger (D/O) warm events (numbered). The timing of Heinrich events is marked in red. Grey lines at intervals of 1,470 years illustrate the tendency of D/O events to occur with this spacing, or multiples thereof [Adapted from Rahmstorf, 2002].

Long glaciations, short deglaciations and secondary rapid transitions are characteristic for every Late Quaternary glacial to interglacial transition [Denton et al., 2010]. Several hypotheses have been brought forth to explain the Late Quaternary glacial to interglacial transition. In the next paragraphs the most accepted and evidenced ones are described starting with the D-O cycles. From this point onwards it continues with the Heinrich events and ends with the glacial to interglacial transition. Note that the AMOC is closely related to these secondary climate transitions.

D-O cycles, first discovered by Dansgaard et al. in 1993, are the most pronounced climate changes that have occurred during the past 120 kyr. They are not only large in amplitude, but also occur quite abrupt. In the Greenland ice cores, D-O events start with an interstadial (a warm period within a glacial); a rapid warming by 5-10°C within at most a few decades, often followed by a plateau phase with slow cooling, lasting several centuries, and ending with a more rapid drop back to cold or stadial (a cold period within a glacial) conditions (Fig. 6) [Rahmstorf, 2002].

The trigger for a D-O event is likely an astronomical forced change in insolation on a sub-milankovitch scale [Broecker, 1994]. In this case, rapid warming in the North Atlantic results from a northward intrusion of warmer subtropical Atlantic waters into the Nordic Seas. These waters induce an increased melting of the Greenland ice sheet, after which the AMOC slows down [Stommel, 1961; Broecker, 1990]. Next, because a reduced AMOC draws less heat from the Southern Hemisphere [Maslin, 2001] the North Atlantic climate cools down causing the plateau cooling in Fig. 6. Reduced deep water formation at the same time forces a salinity build up in the Nordic Seas which potentially restores deep water formation and thus the AMOC after a D-O event [Broecker, 1990]. This process resets the climate to its previous glacial state of ice-buildup.

The fact that the North Atlantic draws heat from the south has already been emphasized in section 1.1. Once the AMOC shuts down, the North Atlantic cools while the South Atlantic warms (Fig. 3). Records from both hemispheres show that this heat piracy [Maslin, 2001; Rahmstorf, 2002] has also taken place during the glacial climate [Stocker, 1998; Denton et al., 2010]. Phase relations show that a change in the North Atlantic always precedes a change in the South with a delay in the order of hundreds to thousands of years. Furthermore this response is reversed with respect to the North Atlantic climate change. The timing of this delay emphasizes the control of the deep AMOC since it is comparable to the residence time of deeper water [Maslin, 2001; Bigg and Martin, 2000; Manabe and Stouffer, 1995]. Evidently, the AMOC transfers a change in insolation into a change in global climate.

D-O events show similar behavior in both glacial and interglacial periods [Maslin et al., 2001; Rahmstorf, 2002]. Nevertheless, the striking difference between both climatic states is the occurrence of Heinrich events within the glacial periods. Heinrich events have been first encountered as distinctive peaks in ice-rafted debris (IRD) within sediment cores of the North Atlantic [Heinrich et al., 1988]. In the North Atlantic they occurred simultaneously with peaks in specific cold polar marine micro-organisms (*N. pachyderma*, *sinistral*) down to latitudes that experience subpolar to tropical climates at present. Proxy records in the Greenland ice cores suggest a further 3-6°C drop in temperature from the already cold glacial climate during these events [Bond et al, 1993; Dansgaard et al, 1993]. Heinrich events are best explained as intense ice rafting pulses primarily related to a collapse of the Laurentide ice sheet [Bond et al., 1999]. Simultaneous cooling in the South Atlantic during the first years of a Heinrich event is presumably related to these pulses.

Heinrich events have been suggested to be caused by a combination of an internal and external forcing mechanism. An internal forcing mechanism could have been triggered at times when northern ice sheets reached a maximum stable volume. At maximum volume, geothermal energy could no longer escape the base of the ice sheet. The only possibility to escape was then by heating the base of the ice sheet resulting in a massive collapse of ice bergs, as explained by the binge-purge model [MacAyeal, 1993].

Another internal forcing mechanism is related to the D-O events. The additional melting in the Nordic Seas during a warm D-O excursion would have increased the regional sea level. An increased regional sea level supposedly calved and thus melted the Laurentide ice sheet from



underneath [Maslin et al., 2001]. This sea level feedback is extremely rapid [Fairbanks, 1989] and sequential D-O surging events might have eventually triggered the threshold for ice collapse.

In relation to the massive discharge of ice bergs, a Heinrich event forced cooling in the South Atlantic and a shutdown of the AMOC. During glacial times with ice coverage extending further south, deep convection sites likely shifted towards the mid-latitude in response to such an event [Rahmstorf, 1994; Toggweiler and Samuels, 1998]. The relocation of deep water formation regions might have initiated a restart of southern heat piracy after an event of total ice collapse [Ganopolski 2001]. This would have restored the AMOC to a pre-Heinrich state.

Another hypothesis which explains the recovery of AMOC after a Heinrich event is related to deep water formation on the Southern Hemisphere. After the initial Heinrich cooling, the South Atlantic warms up due to a shutdown of AMOC, which results in a decrease of AABW formation. This feedback supposedly helped restoring northern deep water formation by forcing an increased pressure gradient towards the North Atlantic [Maslin, 2001]. This hypothesis does, however, imply that is less stable than assumed. Recent evidence suggests that Antarctica might indeed be more subjective to millennial climate change [Cook et al. in 2013].

So far we have seen that D-O events initiated periods of reduced AMOC which had a global climatic impact [Clarke et al., 1999]. Furthermore the D-O events have a pronounced periodicity presumably induced by insolation forcing on sub-milankovitch scale. Also, in glacial times a combination of both several D-O surging events and the binge-purge model, likely preconditioned the northern ice sheets towards a Heinrich event. It, nevertheless, remains remarkable what ultimately drives deglaciation. Furthermore, it is not yet well constrained what mechanism is responsible for a restart of the AMOC after a Heinrich event and/or termination. In the next section these features are further envisaged.

### **1.2.3. The last glacial to interglacial transition: the role of the carbon cycle**

As previously mentioned, a termination event is related to both maximum external forcing and a maximum volume of the northern ice sheets. When ice sheets have reached a volume close to their maximum and a threshold initiates melting, all feedback systems are thrown in reverse [Maslin et al. 2001]. Furthermore, the natural instability of ice sheets implies that ice melt is more rapid than ice growth [Maslin et al., 2001; Ruddiman, 2008]. Still, this does not explain why not every D-O warming triggered deglaciation.

The last warm excursion preceding the deglaciation is the highest recorded over the last glacial period. Moreover, this Allerød/Bølling event occurred immediately after H1. It is thus hypothesized that by the time the YD set in, in response to a shutdown of the AMOC, too much ice had already melted down for ice build-up to resume. Furthermore, a maximum increase in insolation allowed atmospheric CO<sub>2</sub> to rise towards a concentration high enough to provide a strong global warming feedback [Anderson et al., 2009]. The greenhouse level in our present climate stabilizes the northern ice sheet in such a way that Heinrich-like events are prevented from taking place [Maslin et al., 2001].

Summing up, ever since the development of NADW, the AMOC is a major component of the climate system. Whenever insolation changed, the interaction between the northern ice sheets and the AMOC translated this forcing towards a global change in climate. Depending on the magnitude of the trigger the climate system quickly moved from one setting to the other as visualized by figure 4. Every state of climate corresponded to a specific state of AMOC. Although the AMOC is relatively stable at present, it has known different states in the past [Sarnthein et al., 1994; Alley and Clark, 1999].

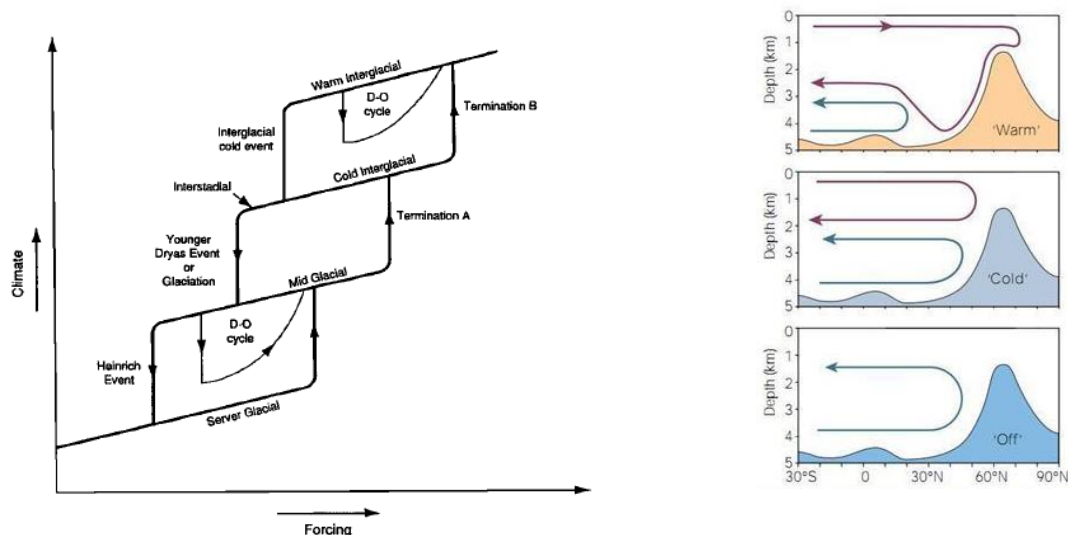


Figure 7 (left) four states of Late Quaternary climate ranging from a severe Glacial to a warm Interglacial. The forcing mechanism (insolation) initiates the climate state through a series of rapid climate transitions. For example, an increased forcing in a severe glacial can move the climate into a mild glacial. Whether or not this happens depends on the occurrence of D-O cycles and a Heinrich event [Maslin et al., 2001]. Right: these transitions closely interact with the AMOC. The ridge in the north represents the sill between the Norwegian Sea and Denmark. A warm overturning corresponds to the present interglacial climate. A cold overturning corresponds to the glacial overturning with NADW further south. An off mode corresponds to a Heinrich event [Rahmstorf, 2002].

Simplified, these can be defined as stadial, interstadial and Heinrich mode. In the interstadial or warm mode, NADW formed in the Nordic Seas. Second, in the stadial or cold mode NADW formation reduced or shifted towards the subpolar open North Atlantic or south of Iceland. Last, in the Heinrich or off mode NADW formation all but ceased and AABW filled the deep Atlantic basin. Still, this theorization is very simplified. Furthermore, evidence that these states in AMOC have indeed occurred is predominantly theoretical. Several phenomena are still very poorly constrained. For example, it is not yet perfectly constrained what drove a change from Heinrich mode back towards a stadial mode or even interstadial mode over a termination event [Voelker et al., 2006].

Several mechanisms have been suggested to be controlling this phenomenon. These ideas, when proven, can fill in the gaps of our understanding of the AMOC and therefore the climate system. In the next chapter one of these ideas, involving the Mediterranean Outflow, is introduced.

## 2. Filling in the gaps: The Mediterranean Outflow

In the previous chapter the control of the AMOC on climate has been emphasized. Studying this control is fundamental in order to develop future climate scenarios. In this view, especially the rapid transitions across the last termination (20-10 ka) are important to investigate.

North Atlantic circulation has played a key role in these rapid climate oscillations [Boyle, 2000] (see section 1.2.2). The strength of overturning reduced by 30-40% in the Last Glacial Maximum (LGM) (20 ka) and completely shut down during H1 (18-15.5 ka) [McManus et al., 2004; Hemming, 2004]. Furthermore, in 1,400 years overturning almost restored to its full capacity, synchronous with the Bølling warming event (14.7-12.7 ka) [Cronin, 1999]. A similar rapid transition from reduced overturning towards interstadial (or warm) overturning took place subsequent to the Younger-Dryas [McManus et al., 2004].

Up to now it remains puzzling how overturning could resume within 1,400 years of a complete shutdown. Furthermore, it is striking that synchronous with this restart, North Atlantic temperatures returned to LGM values. From a physical point of view, the North Atlantic climate can warm only after overturning and thus southern heat piracy has regained its previous strength. Several oceanographic mechanisms have been proposed to explain this remarkable phenomenon.

Unfortunately, a relocation of NADW (section 1.2.2) has up to now not been proven. The same applies for the theory regarding an increase in AABW in response to a Heinrich event (section 1.2.2).

Another mechanism capable of quickly restoring the strength of overturning is one that amplifies the density in the North Atlantic. Especially a re-supply of salinity is crucial in order to remove the freshwater caps after H1 and the YD, since temperatures were already very low due to the melting of icebergs [Stommel, 1961; Broecker, 1990; McManus et al., 2004; Munk & Wunsch, 1998]. It might be that the freshwater cap gradually attracted this warm saline water from the South [van Kreveld et al., 2000]. The accompanied heat would then have additionally warmed the North Atlantic climate. This mechanism would switch the AMOC from an off into a warm mode (Fig. 4).

Salt advection from the Caribbean [Schmidt et al., 2004] and Indian Ocean [Knorr and Lohmann, 2003] has also been proposed to sustain the deep water formation in the North Atlantic during glacial retreat. Yet another density amplification mechanism is proposed to be related to the Mediterranean Outflow (MOW) [e.g. Rahmstorf, 1998; Bigg et al., 2003; Rogerson et al., 2006; Ivanovic et al., 2013].

The earliest hypothesis involving the MOW suggested that upon leaving the Gibraltar Straits, a core of MOW takes a direct northward flow path to the northernmost North Atlantic and GIN Seas, where it provides relatively saline water to convective regions [Reid, 1978, 1979]. Upon cooling, the relatively high-saline waters would contribute towards destabilization of the water column and thus drive local overturning. However, this deep source hypothesis has been disproved by model investigations [e.g. Stanev, 1992; Mauritzen et al., 2001; New et al., 2001] and observational data [e.g. Hill and Mitchelson-Jacob, 1993; McCartney and Mauritzen, 2001; Bower et al., 2002] indicating that a deeper branch of MOW does not reach the Nordic Seas. On top of that, deep convection in the North Atlantic is preliminary controlled by interaction at the air-sea interface [Marshall and Scott, 1999] making the effects of a deep saline influx likely irrelevant.

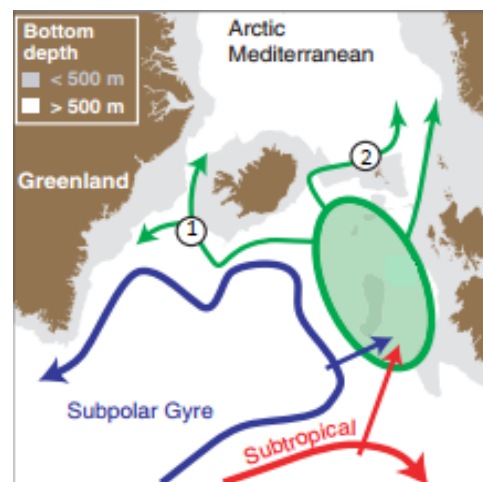


Figure 8: Surface transport across the North Atlantic and the Arctic Mediterranean: the green circle highlights mixing of the subtropical and subpolar gyres after which waters either flow towards the 1) Labrador Sea or 2) the GIN Seas [adapted Hátún et al., 2005].

In response to this evidence, the shallow source hypothesis originated. According to this idea, MOW spreads predominantly westwards along the Iberian Margin and increases the salinity of the north-eastward flowing NAC through mixing at the interface of both the subpolar and subtropical gyre (see Fig. 8) [Hátún et al., 2005]. By increasing the salinity of the NAC, deep water formation intensifies [Kuhlbrodt et al., 2007].

General circulation models (GCMs) generally agree on this mainly westward flow path along the Iberian Margin into the North Atlantic at depth [Rahmstorf, 1998; Bigg and Wadley, 2001; Chan and Motoi, 2003; Rogerson et al., 2010]. They estimated the contribution of MOW to NADW formation at roughly 10% [Rahmstorf, 1998]. However, uncertainty does remain regarding the extent to which MOW is capable of influencing the North Atlantic Current and global climate [Ivanovic et al., 2013].

Nevertheless, there is strong model based [Bigg and Wadley, 2001; Rogerson et al., 2010] and proxy-based [e.g. Rogerson et al., 2006, 2010; Voelker et al., 2006; Penaud et al., 2011] evidence which suggests that across the last glacial to interglacial transition, strengthened MOW provided a negative feedback to North Atlantic freshening boosts quickly rebooting a reduced or inactive AMOC. Penaud et al., 2011 even proposes that MOW could be the trigger for switching between stadial and interstadial AMOC modes. An improved understanding of MOW in relation to overturning across the past millennial climate transitions could thus fill in the gaps in our understanding of the climate system.

This study aims to validate to what extent MOW sustained overturning across the millennial transitions within the last glacial termination. Furthermore it aims to qualify the origin of the presumable changes in MOW strength within this interval. The next chapter contains a full description of the steps undertaken to fulfill these aims.

### 3. Methodology

The approach used to validate the control of MOW on overturning across millennial climate transitions is described in five sections. In section 3.1 both the strategies and studied site are introduced. Next, section 3.2 contains a full description of the applied proxies. In section 3.3 the sampling and proxy recovery is described. Section 3.4 continues with the methodology used to reconstruct bottom water salinity. Last, in section 3.5 the applied age model is explained.

#### 3.1. Strategies and studied site

As mentioned in section 1.1, deep sea sediment cores have been fundamental for paleoclimatologic and oceanographic research. This study thus chose a similar approach. The properties of the MOW have been reconstructed across last glacial termination (0-21 ka) using three deep sea sediment cores.

The cores have been obtained by IODP expedition 339 located off the coast of Portugal close to the strait of Gibraltar. At site U1390 (36°19.110'N, 7°43.078'W) (Fig. 9) three holes, U1390A, B and C, have been drilled at 993,4 mbsl (meters below seafloor) using an advanced piston corer and extended core barrel in order to correct for potential recovery losses. The depositional system at site U1390 has been subjected to very high rates of sedimentation over the past 5 Myrs directly forced by MOW [see chapter 4]. This resulted in a continuous high resolution record of Pliocene to Holocene times. The meters composite depth (mcd) scale for site U1390, which allows correlation of the three holes, has been based on correlation of magnetic susceptibility and natural gamma radiation. The correlation is stated to be relatively straightforward down hole for the studied interval [IODP Proceedings, 2013].

Due to a scarce abundance of benthic foraminifera [see section 3.2; 3.3] the study primary focused on four key intervals: the LGM, H1, S1 and the Late Holocene. A high-resolution reconstruction of the MOW across these intervals both times and verifies the possible control of MOW on the restart of overturning after H1. Furthermore, a reconstruction of MOW across the deposition of S1 (10.8-6.1 ka) [De Lange et al., 2008] provides insight into the relation between deep water formation in the (Eastern) Mediterranean and the strength of (Western) MOW. Moreover, this comparison supplies information regarding the origin of the (proposed) changes in MOW strength across the termination.

For every interval the salinity, temperature and flow strength are reconstructed using several proxies [see section 3.2]. The outcome of these reconstructions is related to the present hydrography of the MOW [see chapter 4].

The next section contains a description of the applied proxies. Note that this study for the first time applied both the Mg/Ca and clumped isotope temperature proxy. At the moment, both proxies still contain significant error margins [see section 3.2]. A combination of both proxies not only provides an accurate reconstruction of temperature but also additional insights into the origin of these error margins.

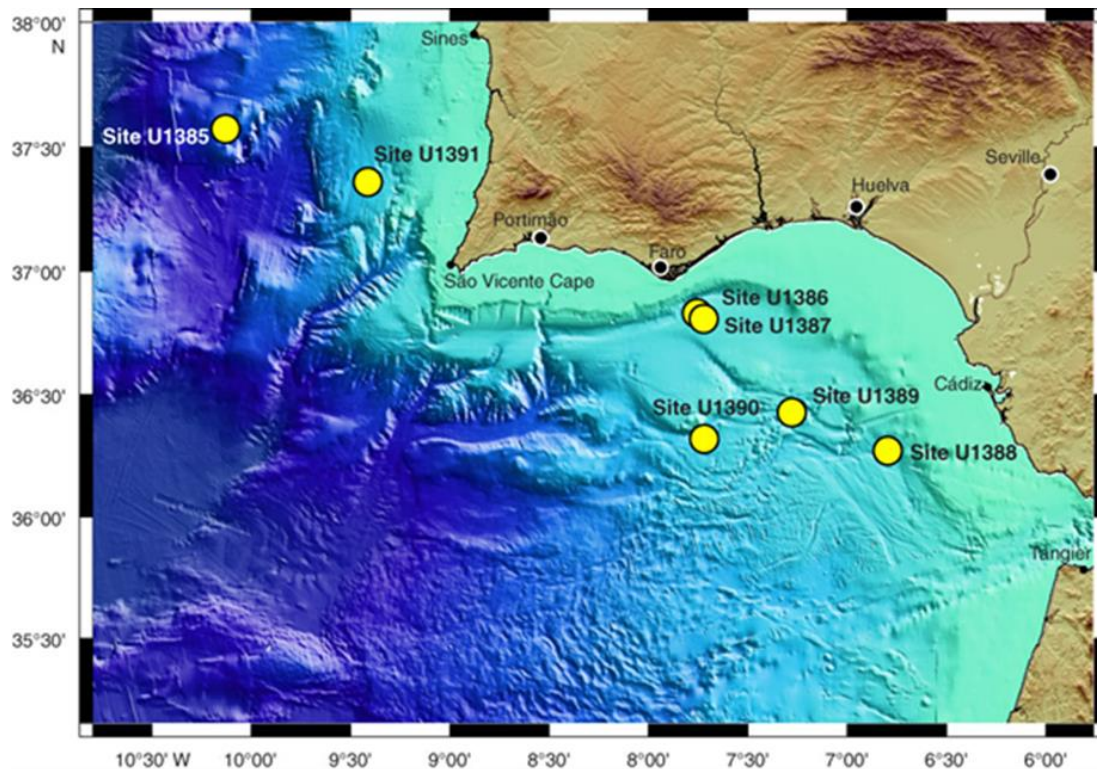


Figure 9: IODP Expedition 399 sites. Site U1390 is located in the Gulf of Cadiz close the Guadalquivir and Guadiana deltas [see chapter 4] [IODP Proceedings, 2013].

## 3.2. Applied proxies

Several proxies are used in order to reconstruct the hydrographic characteristics of the MOW across the termination. In this study especially the remains of marine foraminifera have been analysed. Furthermore, grain size and magnetic susceptibility are analysed to indicate the strength of the MOW. In the next three sub-sections, both proxies involving the shells of marine foraminifera and proxies used to indicate flow strength are introduced.

### 3.2.1. Stable isotopes

The stable isotopic composition of both carbon and oxygen within well-preserved carbonate shells of foraminifera, unicellular marine organisms, has proven to be a decent proxy for environmental change. First, the stable oxygen isotope ratio  $\delta^{18}\text{O}$  is determined by changes in ice volume, local temperature and salinity as first emphasized by Epstein et al., in 1953.

Ice formed on the poles mainly consists of the lighter water molecule,  $\text{H}_2^{16}\text{O}$ , due to physical fractionation of water vapour during transport to the Polar Regions. Therefore, during periods of intense glaciation, the remaining composition of seawater is relatively enriched in  $\text{H}_2^{18}\text{O}$  while the composition of ice on the poles is relatively enriched in  $\text{H}_2^{16}\text{O}$ . The bulk ocean ratio of heavy to light oxygen isotopes,  $\delta^{18}\text{O}_{\text{seawater}}$ , is recorded by marine organisms that produce a test which consists of oxygen like carbonate. This way, records of past precipitated ice and carbonate fossils can be used to reconstruct changes in this ratio and therefore changes in ice volume.

Apart from bulk  $\delta^{18}\text{O}_{\text{sw}}$  as controlled by ice volume, several local environmental parameters also influence the final incorporated ratio; the  $\delta^{18}\text{O}_{\text{carbonate}}$ . Temperature significantly influences the kinetic and physical fractionation which favours incorporation of light oxygen isotopes. Moreover the local evaporation/precipitation balance together with the input of river systems puts another constraint on the amount of heavy to light isotopes available for nutrition. Since the same balance controls the local salinity of the water, the stable isotopic ratio has also been applied as salinity proxy [e.g. Pierre et al., 1999].

Especially in surface waters, the oxygen isotopic composition of calcifying organisms like planktic foraminifera can be locally different. Local river discharge supplies a flux of lighter oxygen and changes the salinity of the water. Moreover, temperature, evaporation and precipitation can vary extremely due to seasonality. This produces 'noise' or high variability in the recorded planktic  $\delta^{18}\text{O}_c$ .

Therefore, when aiming to investigate long-term environmental and climate change, benthic, deep dwelling, and foraminifera have proven to be better candidates. The environments in which these calcifying organisms live are much less influenced by this noise. Environmental parameters are more stable due to the relatively slow buffering flow rate of deep water masses which is the only medium to transfer heat and nutrients. Sudden external fluxes of water do not influence the bulk  $\delta^{18}\text{O}_w$  composition and/ or change the deep water environment.

Second, carbon isotopes have also proven to be decent proxies of several environmental parameters.  $\Delta^{13}\text{C}_c$  is primarily a function of the dissolved inorganic carbon (DIC)- $\delta^{13}\text{C}$  in seawater [Epstein et al., 1953]. On geological time-scales  $\delta^{13}\text{C}_c$  signatures are controlled by changes in carbon sources and sinks (e.g. volcanic outgassing, chemical weathering of continental rocks). On short time-scales  $\delta^{13}\text{C}$  are more regionally controlled by productivity and the mixing of water masses.

Physical fractionation during photosynthesis favours the incorporation of lighter  $^{12}\text{C}$  into the carbonate structure. Therefore, in surface waters with high primary and export production, phytoplankton can deplete the shallowest surface waters of  $^{12}\text{C}$ , resulting in a relatively high incorporation of  $^{13}\text{C}$  in planktic foraminifera. This effect is relatively less pronounced for oxygen isotopes, although corrections have to be applied on several species which are more susceptible to these and other vital effects like pH and light intensity [Shackleton, 1974].

Furthermore, mixing of surface and deep water masses controls the exchange of elements in the water column. It is evident that when the level of mixing increases, ventilation of new oxygen to deeper water increases. The availability of oxygen controls degradation of organic matter. At times of higher ventilation, the  $\delta^{13}\text{C}$  ratio will decrease due to extensive release of  $^{12}\text{C}$ . Therefore the isotopic carbon composition of deep dwelling foraminifera will lighten at times of extensive organic matter degradation. This effect is then further enhanced at times of high surface water primary and export production, resulting in a greater contrast between planktic and benthic  $\delta^{13}\text{C}$ . Apart from that, when the level of mixing is higher, the downward flux of heavy  $^{13}\text{C}$  is higher.

As a result from the above mentioned processes, considerable differences in  $\delta^{13}\text{C}_{\text{DIC}}$  persist throughout the ocean its water masses. For example, modern deep ocean values vary from  $\sim 1,0\text{‰}$  in the North Atlantic to  $-0,5\text{‰}$  in the North Pacific. These differences result from basin-to-basin fractionation caused by a difference in source regions and deep water circulation patterns. Interbasinal  $\delta^{13}\text{C}$  fractionation occurs primarily because of differences in initial nutrient content due to the surface productivity and export. Furthermore deep water  $\delta^{13}\text{C}_{\text{DIC}}$  evolves as a function of the amount of time the water has been isolated from the surface; a longer isolation allows more degradation of organic matter to occur without a resupply of carbon. The distinct  $\delta^{13}\text{C}$  characteristics of different deepwater masses can therefore also be used to reconstruct changes in deep water circulation patterns [Katz et al., 2010].

Note that locally atmospheric  $\text{CO}_2$  concentrations also to some extent control the DIC composition of surface waters.

The extracted  $\delta^{18}\text{O}$  and  $\delta^{13}\text{C}$  ratios give a qualitative view of the mentioned environmental parameters. In order to provide quantitative estimates, empirical relationships have been established [Epstein, 1953] (see section 3.4).

### 3.2.2. Mg/Ca paleothermometry

It is clear that oxygen and carbon isotopes are no proxies for single environmental parameters. This introduces significant problems when applying proxies. For example, only if the ice volume and temperature at a certain time interval are known, the salinity component contained within the  $\delta^{18}\text{O}_c$  ratio can be reconstructed. Ice volume can be reconstructed by estimating the sea level at a certain

time relative to present and establishing a mass water balance equation. It is, unfortunately, impossible to reconstruct past sea level on high resolution, since subtle changes in sea level are not likely to be recorded. Therefore assumptions have to be made which introduce significant errors in the reconstruction of the other components. Moreover, undefined vital effects further increase the error margin. Proxies that record one specific parameter could help lowering this error margin.

A temperature proxy that has been often used in the last decades is the trace elemental composition of the carbonate shell. Especially the incorporation of Magnesium ( $Mg^{2+}$ ) instead of Calcium ( $Ca^{2+}$ ) is presumably controlled by kinetic fractionation [Nurnberg, 1996]. Equation (2) explains the general relationship between temperature and Mg/Ca incorporation.

$$Mg/Ca \text{ (mmol/mol)} = a * e^{(b * T \text{ (}^\circ C))} \quad (2)$$

Several factors have to be taken into account when using Mg/Ca ratios to reconstruct temperature. Most of these factors also apply to other proxies regarding the tests of marine calcifying organisms like the stable isotopes.

The first process that affects proxy applicability, are inter and intra specific differences in the formation of the carbonate shell [Lear et al., 2000]. Vital processes that control the formation of the carbonate shell can be very different for different species. Moreover, variability in Mg/Ca within different chambers from genetically identical specimens is also substantial [de Nooijer, comment]. The reason for this offset is not yet perfectly constrained.

An often used method to deal with inter- and intra-specific differences is by measuring proxy variability in cultures of living foraminifera or sediment core-tops. These cultures consist of living, or recently died, specimens of existing species or species genetically similar to extinct species. Analysis of cultures and specimens in core-tops provides insights into these specific differences and allows the setup of temperature calibrations. Factors 'a' and 'b' in Eq. 2, for example, have different values for different species. The Mg/Ca calibrations used in this study are attached in section 3.4. Also, in order to correct for intraspecific differences several duplicates of one species are analyzed.

A second process affecting magnesium incorporation, similar to oxygen isotopes, depends on the initial bulk Mg composition of the water. The oceanic residence time of minor elements is, however, relatively long (10 Myr for Mg and 1 Myr for Ca), resulting in constant Mg/Ca on timescales of less than  $10^6$  years [Broecker and Peng, 1982]. However, locally, Mg concentrations can be higher depending to the local salinity [Ferguson et al., 2008].

A third problem is preservation and contamination. Diagenetic processes, like recrystallization or regrowth, affect the carbonate structure after deposition and burial. Using tests affected by diagenesis can result in significant errors. Diagenetic affected specimens can be extensively pyritized and/ or yellow-tanned. A common way to prevent these errors is by a careful selection of specimens. Another way is to measure the variability of different chambers, since diagenesis tends to homogenize the carbonate shell [Lear et al., 2000]. The extend of diagenesis, nevertheless, highly depends on the depository system; sites with high clay-rich sedimentation appear to retain their original structures and geochemical signatures, presumably due to quick burial and low porosity [Pearson et al., 2001; Sexton et al., 2006]. Contamination errors can be prevented by careful selection and specific cleaning procedures.

The last process that potentially hampers the applicability of Mg as a temperature proxy is the carbonate ion effect. Studies of trace element/Ca ratios in benthic foraminifera suggest that element partition coefficients ( $D_M$ ) decrease with decreasing calcite saturation state [McCorckle et al., 1995]. When the carbonate saturation state of the water lowers, trace elements are the first ones to dissolve from the carbonate shell.

### 3.2.3. Clumped paleothermometry

Another proxy that potentially serves as a paleothermometer is the 'clumped' isotope proxy. A review by Eiler in 2007 proposes the use of this new temperature proxy based on the state of ordering of rare isotopes in natural materials like carbonate. Clumped isotope paleothermometry is

based on the ratio  $\Delta_{47}$ . This ratio is a measure of the deviation in mass  $_{47}\text{CO}_2$ , which predominantly consists of the rare ‘clumping’ of  $^{13}\text{C}^{18}\text{O}^{16}\text{O}$ , from the ratio expected if isotopes were randomly distributed (Eq. 1). Similar to the stable isotope proxy, a delta notation is used since the concentrations are too low to be measured as a percentage.

$$\Delta_{47} = (R_{47}/R^*_{47} - 1) * 1000 \text{ (‰)} \quad (1)$$

$R_{47}$  is the ratio of mass 47 to mass 44  $\text{CO}_2$  measured in the sample and  $R^*_{47}$  is the ratio of mass 47 to mass 44  $\text{CO}_2$  expected in the sample if all isotopes of O and C were randomly distributed among the different isotopologues, different isotopes of  $\text{CO}_2$ , defined as the ‘stochastic’ distribution. The  $\text{CO}_2$  used to measure  $\Delta_{47}$  is produced by acid digestion of a carbonate mineral, which is similar to extraction of the stable isotopic signal.

Eiler, 2007, states that as temperature of carbonate formation decreases the  $\Delta_{47}$  increases. This is because the zero-point energy differences between isotopologues of the carbonate ion result in multiply-substituted isotopologues being more stable (lower zero-point energy) than isotopologues with zero or one heavy isotope (higher zero-point energy). At high temperatures, the competing effect of entropy promotes disorder in the system and a random distribution of isotopologues. Therefore at low temperature, carbonate mineral have more doubly-substituted isotopologues than would be expected if all isotopes were randomly distributed among the isotopologues (Eq. 2).

$$\Delta_{47} = \frac{0.04371 * 10^6}{T^2} + 0.2004 \quad (\text{With } T \text{ in } ^\circ\text{K}) \quad (2)$$

Note that the clumping of heavy isotopes occurs within the carbonate crystal. In contrast to stable isotopes, clumped isotopes are thus not influenced by global (and local) isotopic differences in the water surrounding the calcifying organism. Temperature reconstructions are thus also less likely to be affected by intra and interspecific differences.

Still, processes like diagenesis could again significantly affect the temperature reconstruction. If the carbonate test recrystallizes after burial, the newly formed carbonate no longer contains the initial temperature signal. Thus similar to Mg/Ca, the carbonate ion saturation at the site potentially affects the value of the proxy. The extent to which the described processes affect the applicability of both the Mg/Ca and the clumped temperature proxy is discussed in section 6.2.

#### 3.2.4. Grain size and magnetic susceptibility

Two additional proxies used in this study are magnetic susceptibility and grain size. Magnetic susceptibility is a measure of the amount of ferromagnetic grains present in the sediment. This amount depends on the continental character of the grains.

Grain size provides an additional indication for the dominant sedimentation process. Although, pelagic ‘background’ sedimentation is dominated by small grains ( $\sim 38\mu\text{m}$ ), vigorous sedimentation is likely dominated by coarser grains ( $\sim 150\mu\text{m}$ ). The next section continues with a description of the sampling and proxy recovery.

### 3.3. Sampling and proxy recovery

Cores have been sampled every 2 cm. Samples have been weighed and freeze-dried prior to measurement of magnetic susceptibility. Magnetic susceptibility has been measured with the Kappabridge KLY-3 at Fort Hoofddijk at Utrecht University.

Samples have been washed, sieved and weighed for the  $>150$ ,  $>63$  and  $>38 \mu\text{m}$  fractions. Samples have been dry-sieved for the  $>212 \mu\text{m}$  fraction in order to obtain the specific foraminifera specimens (and sizes) suitable for further analysis. Since not one single species is present in great abundance throughout the whole record four species, which show significant abundance throughout



the record (Appendix I), have been selected for this purpose; *Uvigerina mediterranea*, *Hoeglundina elegans*, *Cibicides pachyderma* and *Pyrgo spp* (Fig. 10).

Stable isotopes have been measured on 30 specimens of the planktic *G. bulloides* and 5 specimens of the benthic *U. mediterranea*. At least, respectively, 15 and 1 specimens have been selected in samples that did not reach this abundance. Duplicates of *U. mediterranea* have been measured in order to estimate intraspecific variability. Specimens have been washed with an ethanol solution in an ultrasonic bath in order to remove impurities. Samples have then been crushed and dried at 40°C overnight. Dried samples have been weighed prior to mass spectrometry. Stable isotopic values have been extracted with an automated carbonate reaction device Kiel III coupled to a Thermo-Finnigan MAT253 at Utrecht University. Each sample reacted with 103% phosphoric acid ( $H_3PO_4$ ) for 7 min at 70°C. Calibration to the international carbonate standard NBS-19 and in-house standard NAXOS revealed an analytical precision better than 0.05‰ and 0.08‰ for  $\delta^{13}C$  and  $\delta^{18}O$ , respectively.

Mg/Ca ratios have been measured in *U. mediterranea*, *C. pachyderma*, *Pyrgo spp.* and *Hoeglundina elegans*. For Mg/Ca recovery 300µg has been collected per sample from the dry-sieved >212 µm fraction. Mg/Ca samples have been crushed and transferred to a 500 µl Eppendorf. Samples have been cleaned according to Cambridge protocol [Barker et al., 2003] with a few adjustments.

First, a single specimen from every species has been laser ablated with and without adaptation of the cleaning procedure to evaluate to what extent Mn-coatings could be removed; foraminiferal shells from sediments often contain a Mn/Mg oxide-rich coating formed if  $Mn^{2+}$  has been mobilized during anoxic breakdown of organic matter deeper in the sediment column.

The contribution of Mg from coatings to the corresponding Mg/Ca ratio is about 1% [Barker, 2003].

Next, clay and organic removal steps have been performed in a non-acid leached Eppendorf. Furthermore the organic removal step has been performed using  $H_2O_2$  instead of NaOH in order to possibly recover Na/Ca ratios. Samples have been transferred to an acid cleaned Eppendorf prior to the dilute acid leach step. Samples have been cleaned of clay particles with UHQ with three instead of four repetitions. Samples have been rinsed with methanol once instead of twice. Samples have been ultrasonicated once more after removing the overlying methanol. The quality of the remaining material has been evaluated with a microscope. If coarse silicate grains were observed, the remaining material was transferred to a glass plate in order to remove the grains. Mg, Mn, Al, Fe, Na and Ca concentrations have been measured in the dissolved samples with the Thermo Scientific Element-2 at the NIOZ on Texel. Analytical precision for the Mg/Ca measurements is 0.9%. Fe/Mg and Al/Ca ratios have been measured in order to indicate silicate contamination. Fe/Mg and Al/Ca values above respectively 0,1 mmol/mol and 40µmol/mol have been removed [Barker et al., 2003].

In order to apply clumped paleothermometry, 2mg of carbonate is required per sample. Clumped temperature has thus been inferred using stacks of samples. Specimens have been specifically collected within the four intervals of interest and measured in 200µg aliquots [after Schmid and Bernasconi, 2010].

### 3.4. Bottom water salinity estimation

In order to estimate bottom water salinity, empirical relationships have been used which are based on core-top and culture calibrations. The measured Mg/Ca ratios have been used to derive bottom

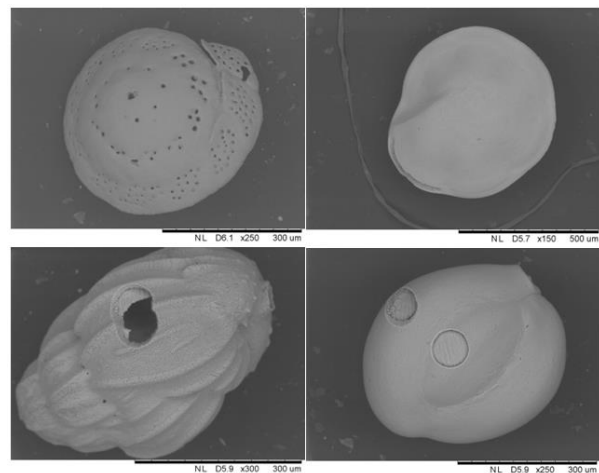


Figure 10: Benthic species used in this study from top left to bottom right: *C. pachyderma*, *H. elegans*, *U. mediterranea*, *Pyrgo spp.* Laser ablation holes are visible in the last two, scale 1cm = 300 µm

water temperatures using Eq. 2 (section 3.2.2). Note that the ‘a’ and ‘b’ factors vary for different species (Table 1).

Next,  $\delta^{18}\text{O}_{\text{sw}}$  (sea water) is derived by correcting for temperature (Eq. 3) [Shackleton, 1974]. This equation is capable of reconstructing temperatures lower than 16.9 °C. The 0.27 factor is required to transfer  $\delta^{18}\text{O}_c$  from the PDB (PeeDeeBelemnite) scale to the SMOW (Standard Mean Ocean Water) scale.

$$T \text{ (}^\circ\text{C)} = 16.9 - 4.0 (\delta^{18}\text{O}_c - (\delta^{18}\text{O}_{\text{sw}} - 0.27)) \quad (3)$$

**Table 1: Mg/Ca calibrations used in this study**

Species	a	b	Source
<i>Cibicides spp.</i>	0,90 ± 0,037	0,11 ± 0,003	Elderfield et al., 2006
<i>Uvigerina spp.</i>	0,94 ± 0,044	0,053 ± 0,004	Elderfield et al., 2006
<i>H. elegans</i>	0,21	0,23	Cappelli et al., unpublished
<i>Pyrgo spp.</i>	5,5	0,16	De Wit et al., 2012

Third,  $\delta^{18}\text{O}_{\text{sw}}$  values have been corrected for ice volume [Waelbroeck et al., 2002]. The resulting ice volume free  $\delta^{18}\text{O}_{\text{ivf-sw}}$  value reflects changes in salinity. Using a salinity relationship established for the Mediterranean Sea (Eq. 4)  $\delta^{18}\text{O}_{\text{ivf-sw}}$  is translated into paleo-salinity [Pierre, 1999].

$$\delta^{18}\text{O}_{\text{ivf-sw}} = 0.27 * S - 8.9 \quad (4)$$

Equations 3 and 4 have been evaluated using the recent salinity at site U1390 which is roughly ~36 ‰ [IODP Proceedings, 2013]. Using core-top  $\delta^{18}\text{O}_c$  data, a temperature of 11.5 °C has been derived which is quite similar to the site temperature of ~12.5 °C [IODP Proceedings, 2013].

### 3.5. Age model

Fifteen  $^{14}\text{C}$  dates extracted from planktonic foraminifera [Ducassou et al., unpublished] have been used to establish an age model (Fig. 11) using Calib 6.0.1 [Stuiver et al., 2010]. The  $^{14}\text{C}$  dates have been corrected for a reservoir age of 400 yrs. No specimens of *Neogloboquadrina pachyderma* (sinistral) have been encountered, although this species has been repeatedly used to indicate cold climate transitions (e.g. H1, YD) in the Gulf of Cadiz [e.g. Voelker et al., 2006; Toucanne et al., 2006]. Tuning of both the  $\delta^{18}\text{O}_{\text{plankton}}$  (*G. bulloides*) to the GISP2 record [Grootes et al., 1999] and the  $\delta^{18}\text{O}_{\text{benthos}}$  (*U. mediterranea*) to the LR04 stack [Lysiecki and Raymo, 2004] indicated that no further adjustments of the age model were required (Fig. 12).

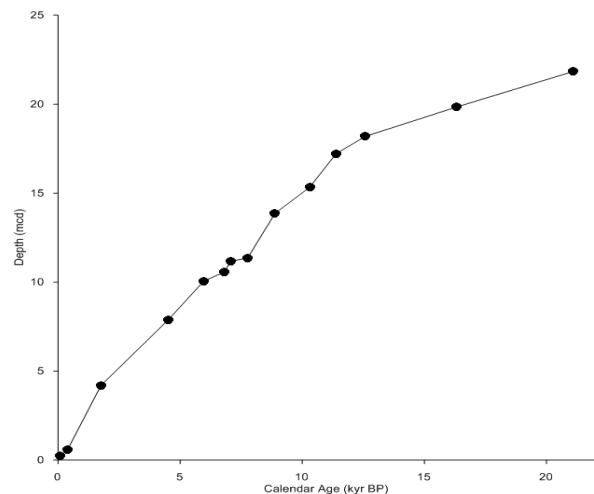


**Figure 11: Age model constructed using fifteen  $^{14}\text{C}$  dates extracted from planktonic foraminifera [Ducassou et al., unpublished]. Depths are in meters composite depth scale.**

## 4. Modern hydrography

At present MOW is a warm (13°C) and saline (38‰) [Bryden and Stommel, 1982] fed by two varying deep water masses; the Levantine Intermediate Water (LIW) and Western Mediterranean Deep Water (WMDW) (Fig. 12). LIW is formed in the eastern Mediterranean basin, and flows across the Strait of Sicily into the western basin [LaFuente et al., 2007]. WMDW is formed in the Gulf of Lions in the western Mediterranean and occupies the bottom layer of the MOW contributing to an estimated 10% [Kinder and Parilla, 1987; Tomczak and Godfrey, 1994] of the total 1 Sv outflow volume [Bryden and Stommel, 1984]. Both water masses are formed in winter when cold dry air from the European continent induce surface water cooling and deep convection in the Gulf of Lions (for WMDW), in the southern Adriatic Sea, in the Southern Aegean Sea, and in the Levantine Basin between Rhodos and Cyprus (for LIW) [Candela, 2001]. Fluctuations in the physical characteristics and volume of the MOW result from the interannual to decadal variability in both water masses [Candela, 2001; Astraldi et al., 2002].

As the MOW enters the Atlantic Ocean through the Strait of Gibraltar it sinks down due to its high density and entrains the North Atlantic Central Water (NACW). This results in an increase in transport volume up to  $2.00 \text{ ms}^{-1}$  [Kinder and Bryden, 1987] and decrease in density; forming a new watermass; the Mediterranean undercurrent [Ambar and Howe, 1979; Baringer and Price, 1997]. Due to its modification after entering the Atlantic Ocean, the MOW's hydrodynamic and energetic behavior is affected which results in lateral spreading [Baringer and Price, 1997]. Possibly along with the variable bathymetry, the MOW splits into two stability levels: an upper core with an initial flow speed of  $1.00 \text{ ms}^{-1}$ , roughly centered between 500 and 800 meter, Mediterranean Upper water (MU), and a more saline and denser lower core between 1000 and 1400 meter with a flow speed of  $0.05\text{-}0.01 \text{ ms}^{-1}$ , called the Mediterranean Lower water (ML) (Fig. 12) [Ambar et al., 2002]. The lower core is mainly fed by WMDW, and the upper core by LIW. Since the studied site is situated at a depth of 993.4 meters below sea level, the study is likely to reflect only changes in the composition of the ML.

At large depth, the MOW locally loses contact with the seafloor in places and spreads over the NADW, before continuing westward and northward into the North Atlantic [Iorga and Lozier, 1999]. The high density and speed of both core currents results in erosion of the seafloor sediments lateral to the strike of the continental slope. This erosion shapes the seafloor in the Gulf of Cadiz and induces the formation of contourites and sheeted sediment drift bodies, like the Faro Drift south of Faro [Faugères et al., 1984; Habgood et al., 2003].

The drift sediment bodies and the average grain-size of sea floor sediments mirror the variability of MOW hydraulic energy [Mulder et al., 2003]. Previous studies suggest that vertical variations of average grain-size in individual contourite beds are records of bottom-current variations [Voelker et al., 2006]. Consequently coarse-grained contourites are interpreted as deposits of increased MOW velocity [Voelker et al., 2006]. Note that the variability in the flow path of the MOW will result in periods of high and low sedimentation. Moreover, discharge from the Guadalquivir and Guadiana deltas could significantly influence the sedimentation at the site [Kaboth, comment]. An increase in continental discharge is likely recorded in a similar way as an increase in MOW intensity by both flow strength proxies.

Although the MOW experiences entrainment of NACW, it maintains a relatively high salinity and temperature, traceable into the open Atlantic and northward along the European continental margin where it, as already mentioned, mixes with both North Atlantic gyres (Fig. 8).

The NACW at a water depth between 100 and 500 meter has two source regions: a warmer and more saline subtropical (st) NACW is formed in winter along the Azores front at 35-36°N and a subpolar (sp) NACW by winter cooling in the eastern North Atlantic north of 46°N [McCartney and Talley, 1982]. NACWst flows eastwards towards the Iberian margin and forms a poleward subsurface current along the Portugues margin [Haynes and Barton, 1990]. Underneath the NACWst the NACWsp can move as far south as 30-35°N [McCartney and Talley, 1982]. As both subsurface currents are formed close-by, oxygen draw down related to water mass aging or high organic matter

fluxes in the upwelling zones off western Iberia and Morocco is relatively small and no oxygen minimum zone persists in the Gulf of Cadiz [Locarnini et al., 2002]. In winter, the surface water in the Gulf of Cadiz consists of subtropical water derived from the Azores Current [Peliz et al., 2005]. The main surface water current, however, follows the northern coastline and transports water from the Portugal Current into the Mediterranean where it balances the volume lost by the outflow. Volumes of inflow are higher than outflow due to a lower salinity of the Portugal Current (~36‰).

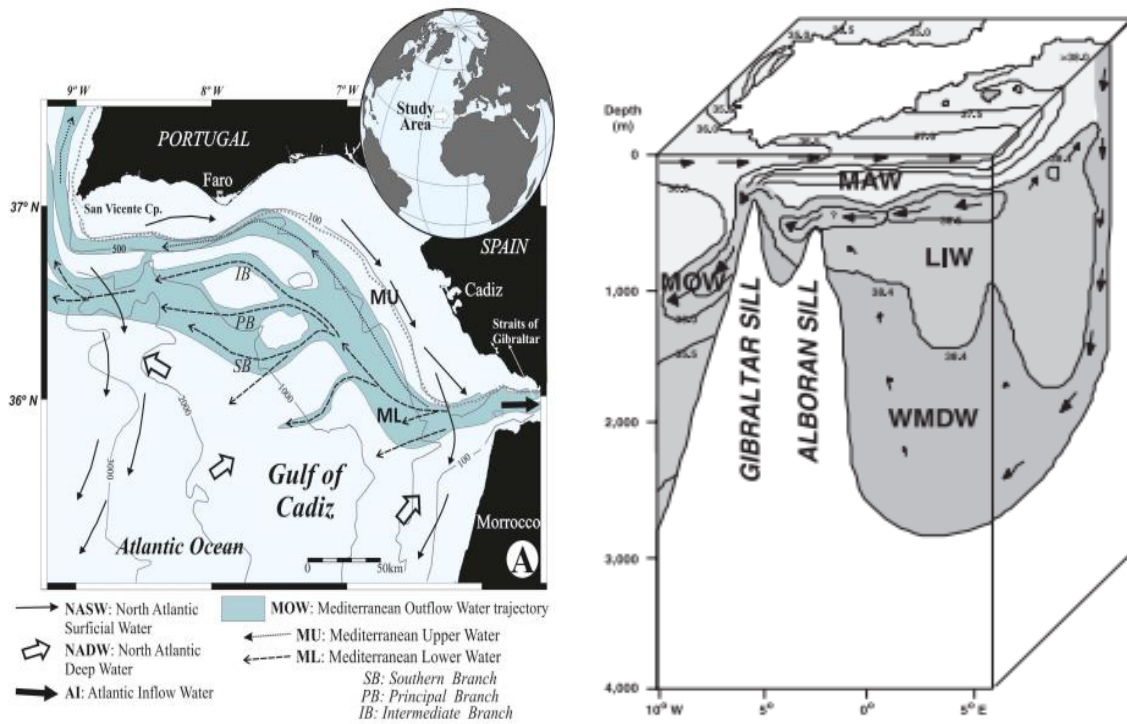


Figure 12: left: modern hydrography of the Gulf of Cadiz with incoming surface waters from the South (Azores Current) and the North (NACW<sub>st</sub> and NACW<sub>sp</sub>) [adapted from Hernández-Molina et al., 2006]. Right: origin of the MU and ML, respectively LIW and WMDW [Cacho et al. 2005]

## 5. Results

### 5.1. Stable isotopes

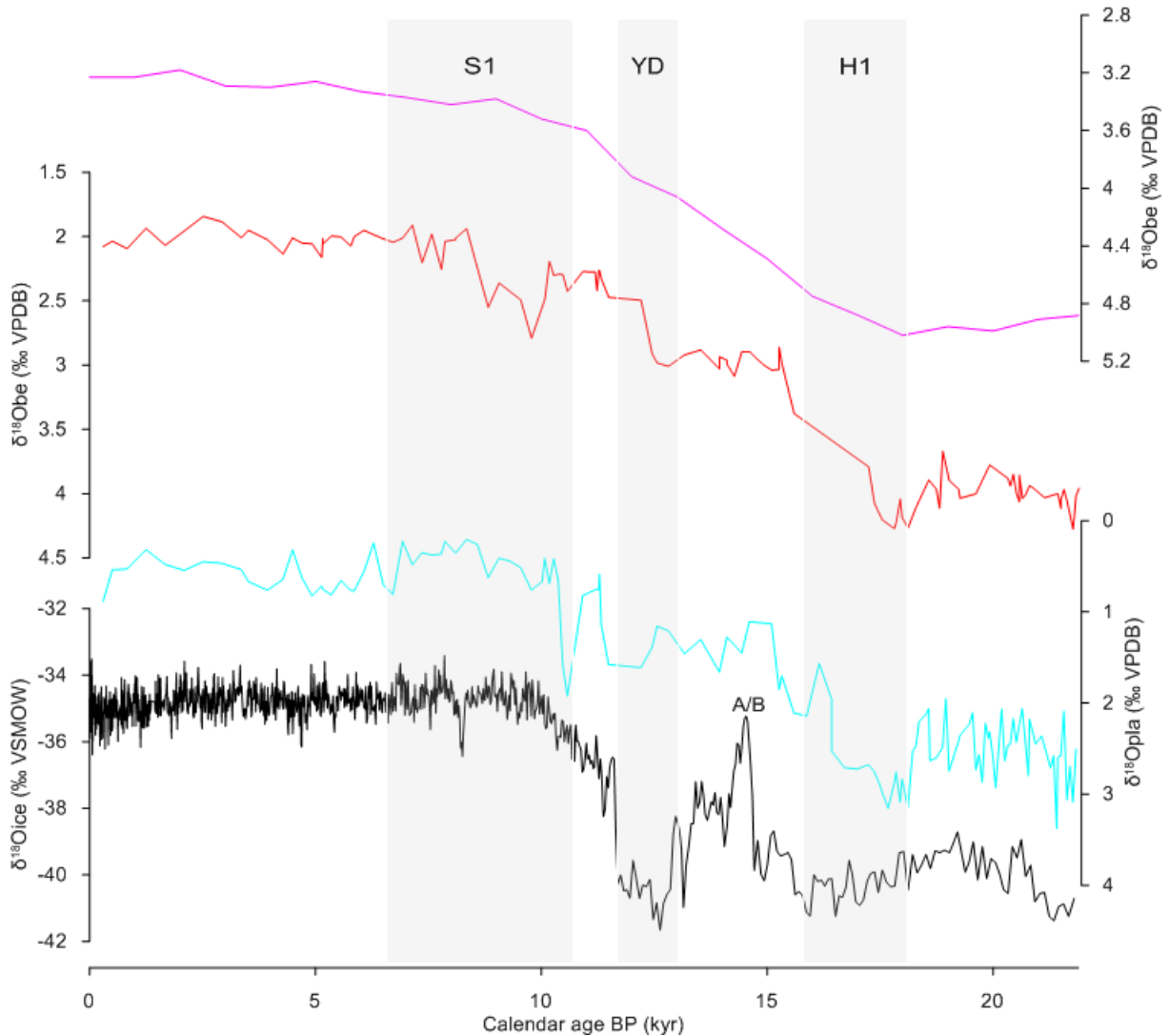


Figure 13: Paleoclimate records of core ODP1390 from the Gulf of Cadiz in comparison with the LR04-stack (purple) and the GISP2 record (black). The benthic  $\delta^{18}\text{O}$  record is based on *U. mediterranea* (red). The planktic  $\delta^{18}\text{O}$  record is based on *G. bulloides* (light blue). H1, YD and S1 are indicated in light grey.

Figure 13 shows both the benthic and planktic oxygen records plotted with the GISP2 record and LR04 stack. Note that duplicates of *U. mediterranea* indicated no significant intraspecific variability. Both planktic *G. bulloides* and benthic *U. mediterranea* records show a clear transition to significant lighter  $\delta^{18}\text{O}$  values, of respectively 3‰ and 2.5‰ across the last termination. The planktic  $\delta^{18}\text{O}$  records show a millennial scale variability of 1‰ in the Glacial compared to a variability of 0.5‰ in the Holocene. The termination initiates with a minimum in  $\delta^{18}\text{O}$  which is closely tied to the occurrence of H1. The associated drop in benthic  $\delta^{18}\text{O}$  is roughly halved with respect to the planktic signal. Moreover, the benthic community shows a shift from abundance in *U. mediterranea* in the Holocene towards *Pyrgo spp.* in the glacial [Appendix I]. Benthic  $\delta^{18}\text{O}$  decreases simultaneous with the deposition of S1 in the Eastern Mediterranean. Also a rapid excursion of planktic  $\delta^{18}\text{O}$  is observed at the start of S1. Furthermore a slight increase in planktic  $\delta^{18}\text{O}$  occurs closely tied to the northern Bølling warming.

Figure 14 shows the benthic and planktic  $\delta^{13}\text{C}$  records together with magnetic susceptibility and the silt/clay ratio. Note that both  $\delta^{13}\text{C}$  records show large scatter. Nevertheless, across H1 a peak in  $\delta^{13}\text{C}$  of *G. bulloides* is observed. A minimal increase in silt sedimentation is observed in the same interval. Furthermore, a gradual rise in planktic  $\delta^{13}\text{C}$  is observed within the Holocene.

The benthic  $\delta^{13}\text{C}$  moving average (5 steps) shows great scatter in the Glacial although a significant drop of 0.5‰ is observed at the start of S1 deposition; a moving average of 5-years is therefore added. The minimum in  $\delta^{13}\text{C}$  of *U. mediterranea* correlates well with the peak in the silt sedimentation. Moreover, the gradual drop and rise in both proxies is also simultaneous. Both records, however, also show intervals of less pronounced and not matching variability. Possibly, a less pronounced peak in silt sedimentation corresponds to the A/B warming event.

Magnetic susceptibility values show an overall increasing trend over the last 20 kyrs. One significant peak appears to match the decrease in the  $\delta^{18}\text{O}$  of *U. mediterranea* across H1.

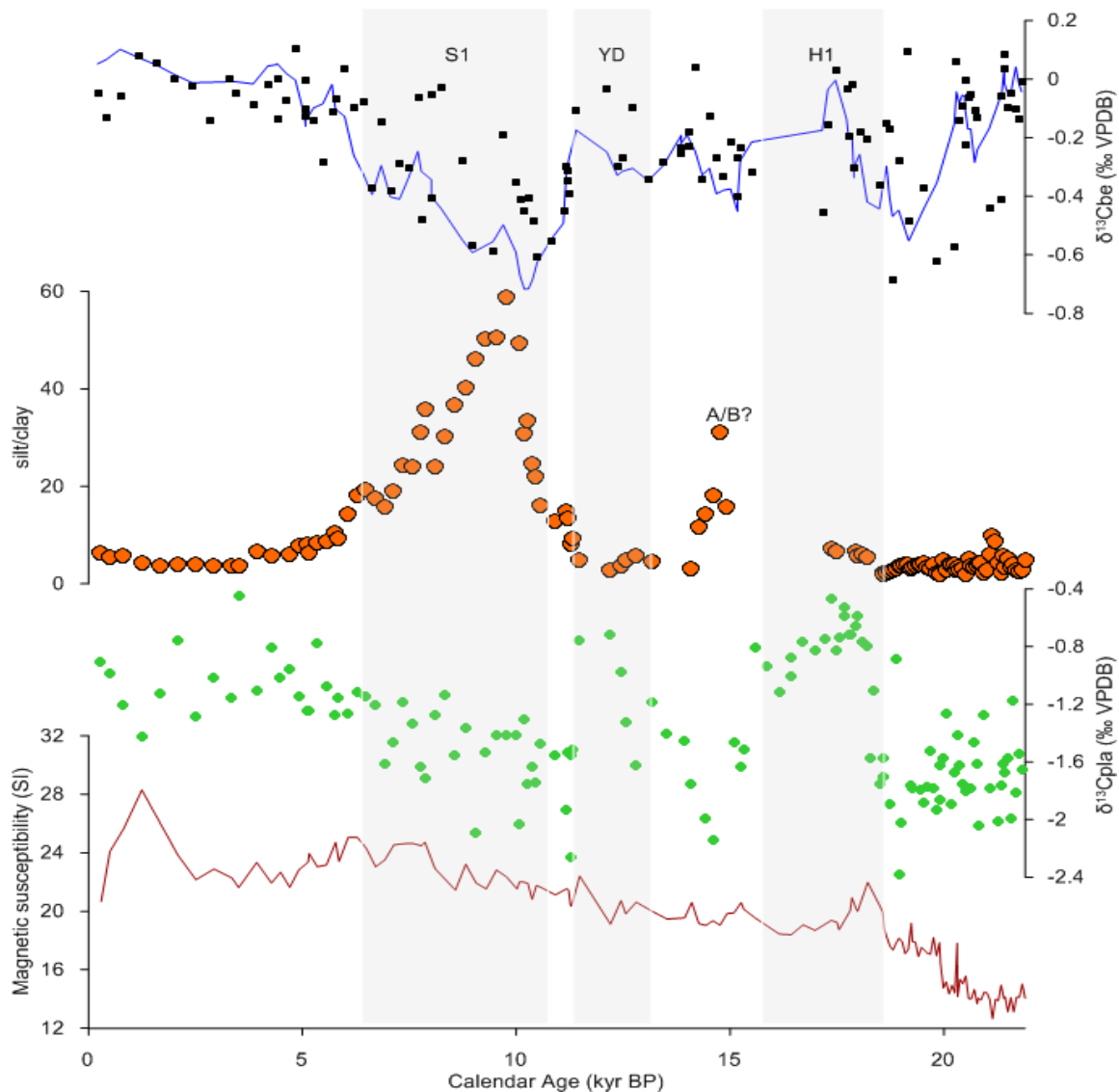


Figure 14: Continued paleoclimate records of core ODP1390 from the Gulf of Cadiz. The  $\delta^{13}\text{C}$  from *G. bulloides* is shown in green.  $\delta^{13}\text{C}$  from *U. mediterranea* (black) is plotted with a 5-sample-moving average (blue). Changes in grain size and sedimentation are revealed by the silt/clay ratio (orange) and magnetic susceptibility (brown).

## 5.2. Bottom water temperature and salinity

Measured Mg/Ca ratios of *U. mediterranea* and *C. pachyderma* are strikingly similar, ranging from, respectively, 0.8-2.5 and 1.0-2.5mmol/mol. *H. elegans* covers a similar range from 0.6-1.2mmol/mol (not shown). Unfortunately, due to equipment failure, only 75% of the Mg/Ca ratios of *Pyrgo spp.* has been recovered. Mg/Ca estimated in this species covers a much broader range from 70-95mmol/mol.

The derived bottom water temperatures (Fig. 15) show a quite consistent pattern. Although there is no deep water temperature trend over the glacial to interglacial transition, there are two pronounced drops in temperature across H1 and S1. Averaged temperatures indicate another drop in temperature synchronous with the cold YD in the Greenland ice record.

*U. mediterranea* temperatures are more scattered than *H. elegans* and *C. pachyderma*. Temperatures extracted from *Pyrgo spp.* are almost doubled with respect to the other species [Fig. 19]. The applicability of *Pyrgo spp.* (and the other benthics) is discussed in section 6.1.

Temperatures extracted using clumped isotopes show a doubled standard deviation with respect to the Mg/Ca temperature estimates. Furthermore, Holocene samples reveal substantially different temperatures using both paleothermometers.

In order to measure the  $\delta^{18}\text{O}_{\text{sw}}$  a composite deep water temperature moving average (Fig. 15) has been used including all species but *Pyrgo spp.* The standard deviation for the composite is roughly 0.5°C based on the standard deviations in the measured duplicates.  $\delta^{18}\text{O}_{\text{ivf-sw}}$  values increase towards the glacial (Fig. 16) implying a higher salinity in the glacial (Fig. 17). In the next chapter the presented results are further evaluated and discussed.

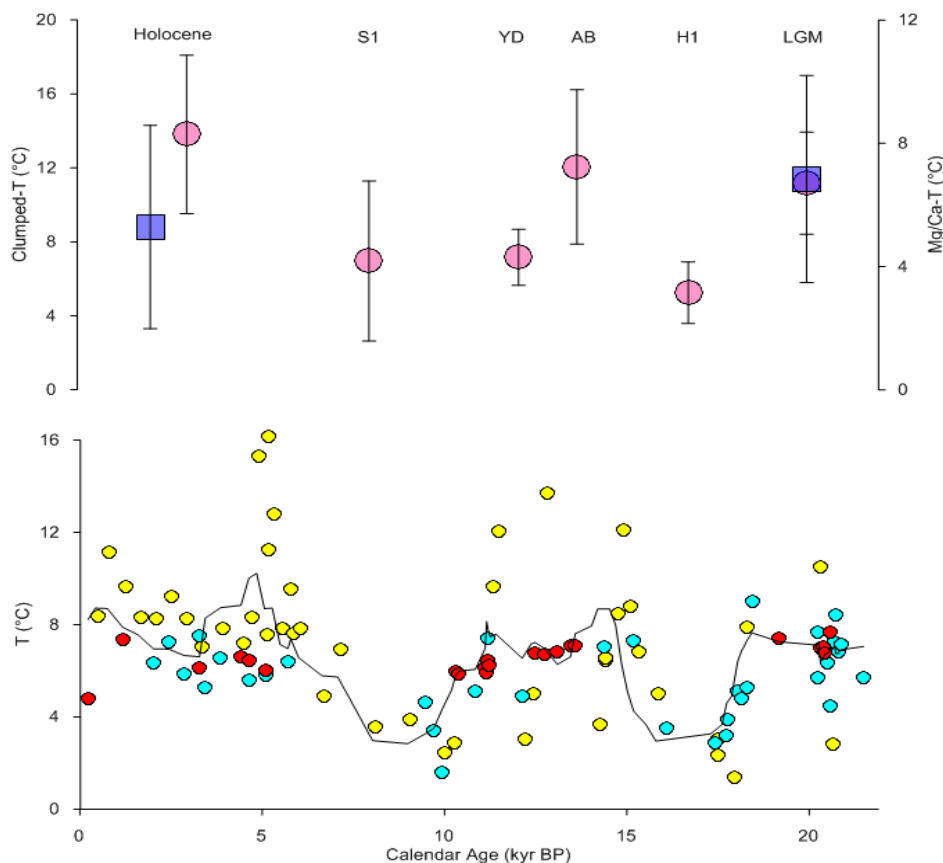


Figure 15: Bottom water temperatures at ODP1390. Top: averages for 6 time slices; Glacial, H1, A/B, YD, S1 and Holocene (see also Appendix 2). Note: Mg/Ca temperatures are presented in pink, clumped temperatures are presented in purple. Bottom: Mg/Ca derived temperatures of *U. mediterranea* (yellow), *C. pachyderma* (light blue), *H. elegans* (red) plotted with a 5-point moving average.

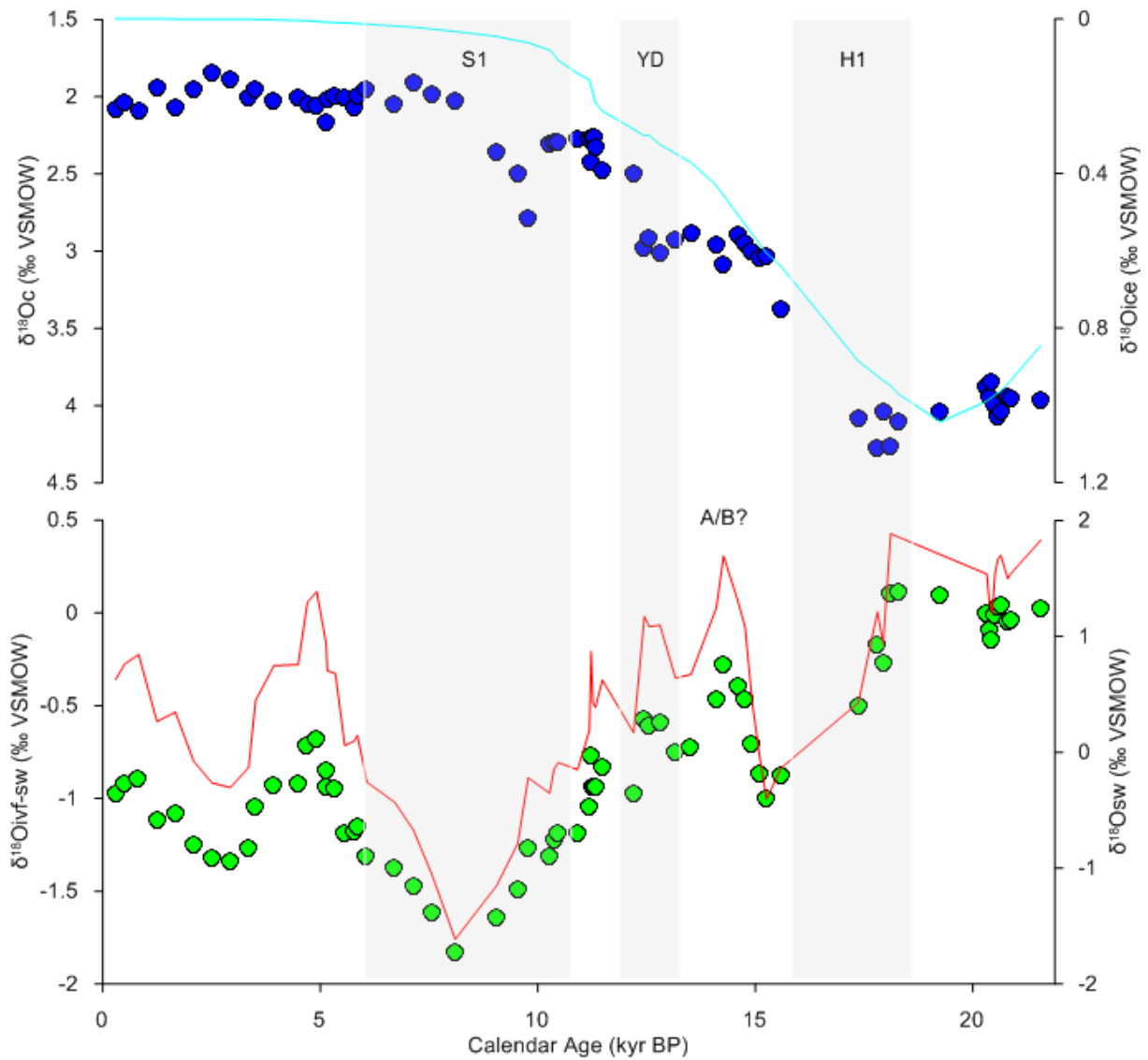


Figure 16: Bottom water salinity determination.  $\Delta^{18}\text{O}_c$  from *U. mediterranea* (dark blue) is used to derive  $\delta^{18}\text{O}_{sw}$  (green) with the averaged bottom water temperatures based on Mg/Ca ratios. Subtracting the ice volume component (light blue) revealed the ice volume free component (red). High  $\delta^{18}\text{O}_{ivf-sw}$  corresponds to increased salinities.

## 6. Discussion

The reconstructed bottom water temperature shows two pronounced drops across H1 and S1. The Holocene temperature average is, however, centred at 8°C. This is in dispute with the present bottom water temperature at the studied site (~13°C). An offset of 5°C appears consistent with reconstructions based on *C. pachyderma* in the Western Mediterranean [Cacho et al., 2006]. Inspired by Cacho et al. in 2006, reconstructed bottom water salinity with and without an addition of five degrees to the 5-point average temperatures (Fig. 15) is revealed in figure 17. Strikingly, the corrected salinity reconstruction indicates a Holocene salinity which is similar to the present salinity at the site (36‰). In the next section, the offset in the temperature record is investigated in order to assess the accuracy of the reconstruction. Only then, analysis and interpretation of events across the termination is possible [section 6.2].



## 6.1. Problems involving the temperature reconstructions

As emphasized in section 3.2, the trustworthiness of temperature reconstructions is potentially hampered in several ways. In this section several of these processes [see section 3.2.2] are evaluated in order to assess the quality of the presented temperatures starting with the Mg/Ca estimates.

### 6.1.1. Cleaning protocol

The first problem that affects the Mg/Ca temperatures is inherent to the cleaning protocol itself. Reviews of benthic Mg/Ca calibrations [Martin et al., 2002; Elderfield et al., 2006; Bryan and Marchitto, 2008] suggest that significant errors are incorporated into the measured ratios when slightly different cleaning protocols are applied. Although the cleaning protocol used in this study is most commonly used, some problems are still partly unresolved.

According to Barker et al., 2003, both silicate minerals and Mn/Mg coatings could significantly affect the extracted Mg/Ca ratios.

First, clay minerals which intrude the carbonate shell contain between 1 to 10% Mg by weight. In order to estimate the level of silicate contamination, as mentioned in the methodology section, one could analyse the covariance between Mg/Ca, Fe/Ca or Al/Ca down-core. According to Barker et al. in 2003 Fe/Mg concentrations exceeding 0.1mmol/mol should always be removed. Al/Ca concentrations above 40 $\mu$ mol/mol also indicate significant amounts of silicate contamination. These ratios have been established based on *G. bulloides* [Barker et al., 2003] but seem to work well for *U. mediterranea*, *H. elegans* and *Pyrgo spp*; samples with Fe/Mg ratios larger than 0.1mmol/mol have been disregarded. Only for *C. pachyderma*, although all Al/Ca measurements are lower than 40 $\mu$ mol/mol, Fe/Mg values are predominantly centred between a ratio of 0.1 and 0.2 mmol/mol [Appendix 2]. Nevertheless, laser ablation trails indicate that the cleaning protocol is capable of removing the silicate Mn coating. Since the temperature trend revealed by *C. pachyderma* is consistent to both *U. mediterranea* and *H. elegans* no samples have been disregarded for the 5-point moving average.

Second, Mn and Mg-oxide coatings, which are formed when Mn or Mg is mobilized during anoxic breakdown of organic matter deeper in the sediment column, can contribute about 1% to the extracted Mg/Ca ratio. Only a reducing agent is capable of removing this coating. This reducing agent is, however, also corrosive to carbonate and causes partial dissolution. This reduction step in the protocol is therefore not applied. One percent contribution is however not enough for 5 degrees offset [Barker et al., 2003]. Recorded Mn/Ca concentrations in *C. pachyderma* and *U. mediterranea* are 100 times higher than in tests from the Alboran Sea bottom waters, although Fe/Ca ratios are of a similar magnitude [Cacho et al., 2006]. Nevertheless, no linear relationship between Mn/Ca and Mg/Ca has been revealed, suggesting no substantial Mg contamination.

It is thus concluded that although the cleaning protocol might affect the reconstructed bottom water temperatures, it is not likely solely responsible for a 5 degrees offset. Since Sr/Ca ratios are less affected by contamination they have been suggested as a proxy for contamination [Rosenthal, 1997]. Unfortunately, Sr/Ca ratios have not been measured in this study.

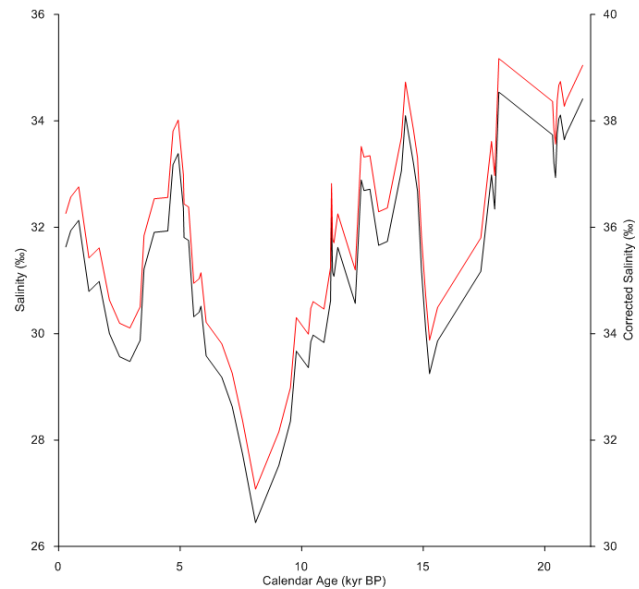


Figure 17: Bottom water salinities at site ODP1390. The corrected salinities (red, right) provide a better match to recent salinities.

Still, not all contamination can be removed with the cleaning protocol. According to Marchitto et al., 2007, the exponential relationships used for *U. mediterranea* and *C. pachyderma* are based on core-top specimens affected by diagenetic overgrowth. These core-tops were located on shallow marine carbonate platforms. At these sites, dissolution and recrystallization of metastable aragonite and high-Mg biogenic calcites occurs during the earliest stages of sedimentation [Hover et al., 2001]. In the oversaturated pore waters of the carbonate platforms, these processes can result in secondary precipitation of high-Mg and high-Sr coatings on foraminiferal tests, thereby changing the primary Mg and Sr composition toward higher values [Rosenthal, 1997]. Although diagenetic overgrowth has likely affected the applied calibrations (read: *U. mediterranea* and *C. pachyderma*), there is no indication of the magnitude. Note that additional diagenesis at the site is minimal considering the high preservation of carbonate under rapid clay sedimentation [Katz et al., 2010].

### 6.1.2. Calibrations

The applicability of the Mg/Ca paleothermometer is also affected by the choice of a calibration. Core-top and culture experiments fundamental in order to derive empirical relationships are all performed under a different set of environmental parameters. It is thus a priori questionable to what extent the applied calibrations match the environmental conditions at the studied site.

Furthermore there are very few calibrations for individual genera. Several different calibrations for *Cibicides spp.* and *Uvigerina spp.* exist based on specimens from the Little Bahama Banks (LBB) [e.g. Rosenthal et al., 1997; Martin et al., 2002; Lear et al., 2002; Marchitto et al., 2003]. It is questionable to what extent these calibrations are applicable on *C. pachyderma* and *U. mediterranea*. According to Elderfield et al. in 2006, calibrations using mixed species of a genus introduce significant errors when applied on individual genera.

In the next paragraphs the four applied calibrations are further evaluated. Note that incorporation of Mg/Ca in benthic species is related to habitat. This section is therefore split up in an in and epifaunal subsection.

#### *Epifaunal species*

Although the temperature calibration applied on the epifaunal species *C. pachyderma* is possibly affected by diagenetic overgrowth, the estimates are very consistent with *H. elegans*. Furthermore, other calibrations for *Cibicides spp.* do not significantly alter this reconstruction [Martin et al., 2002; Lear et al., 2002; Elderfield et al., 2006; Cacho et al., 2006].

Marchitto et al., 2007 provided a relationship for a temperature range of 5.8-18.6 °C based on overgrowth-free specimens applying the same cleaning protocol. Temperatures reconstructed with this calibration are shown in Fig. 18.

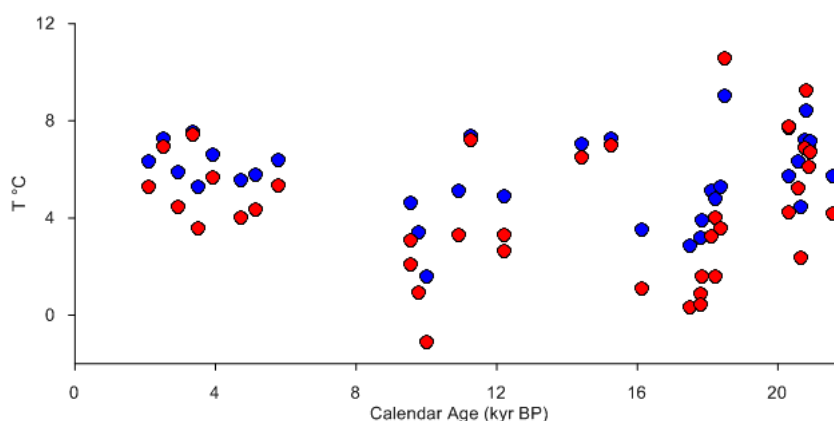


**Figure 18: Bottom water temperatures extracted from *C. pachyderma*. Unlike the Elderfield et al., 2006 calibration (blue), the Marchitto et al., 2007 calibration (red) provides negative temperature estimates.**

At present NADW in the Gulf of Cadiz has a salinity of 35.5‰ and temperature of approximately 5.5°C [Criado-Aldeanueva et al., 2006]. If indeed MOW intensity drops across H1 and S1

temperatures are not likely reach values near freezing point. The Elderfield et al., calibration thus provides a better match to the NADW temperature range. If the calibration is, however, off by 5 degrees, and NADW intruded the site during H1 and S1 with a similar temperature and salinity, the Marchitto et al., 2007 calibration might provide a better candidate. Nevertheless, on the whole, the offset between both records remains relatively minimal, so the Marchitto calibration is disregarded.

Studies have also aimed on to evaluate the applicability of Mg/Ca thermometry in *H. elegans*. Rosenthal et al., 1997, finds that Mg content of *H. elegans* is about half of that found in calcitic species, which is similar to the findings in this study. This is caused by the aragonitic mineralogy which likely incorporates less Mg. A calibration set up by Reichart et al., 2010 provides a similar range of temperatures. The Rosenthal et al., 2006, calibration, however, indicates unrealistic temperatures of around -27°C, which has also been acknowledged by Flaithearta et al., 2010. It could be that the use of a reductive step in this study during the leaching phase preferentially removed high Mg phase from the more soluble aragonitic shells [Flaithearta et al., 2010].

Furthermore diagenetic contamination is minimal in *H. elegans* relative to calcitic species because of the test's smooth and glassy surface [Boyle et al., 1995; Marchitto et al., 1998]. This is also concluded from the low Fe/Mg and Al/Ca concentrations in *H. elegans*. A problem involving *H. elegans*, however, is its high susceptibility to dissolution due to the fact that the aragonite compensation depth is relatively shallow. Apart from the fact that this explains the low abundance throughout the record, partial dissolution of carbonate and aragonite tests results in a lowering of the Mg/Ca ratio since the Mg-enriched carbonate dissolves preferentially [Brown and Elderfield, 1996]. The used specimens, however, did not provide any indication of dissolution.

Nevertheless, it is remarkable that the correlation between both species is so high. Although the temperature documented for the *C. pachyderma* calibration is centred around 13 degrees, the temperature range for *H. elegans* is documented at 3-8°C. Additional measurements on smaller samples of *H. elegans* might provide more insights into this interesting feature.

### Infaunal species

As mentioned in section 5.2, temperatures extracted from *Pyrgo* spp. (Fig. 19 blue) have not been included in the 5-point moving average. The revealed temperatures do not show any correspondence to the general trend.

According to de Wit et al., 2012, the temperature calibration for *Pyrgo* spp. covers a temperature range from 2.4-10.8°C. Furthermore, the Mg/Ca concentrations in their samples ranged from 7-50mmol/mol. There is thus a significant offset with the specimens used in this study ranging 70-90mmol/mol Mg/Ca. It is therefore very likely that the calibration by Wit et al., 2012 is not applicable on the studied site.

A similar study by Toyofuku et al., in 2000 on the miliolid species *Quinqueloculina yabei* proposes a relationship between 10-24°C, which is closer to the temperature at the studied site. Extracted Mg/Ca ratios from cultured and sampled specimens ranged from 90-140mmol/mol. Bottom water temperatures reconstructed using this calibration fit better to the range suggested by the other species (Fig. 19 green). This again proves that when applying calibrations established elsewhere, environmental

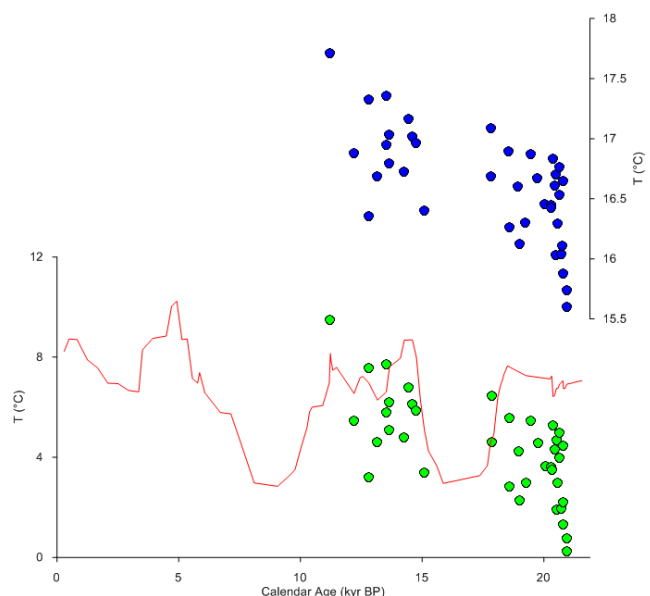


Figure 19: Bottom water temperatures extracted from *Pyrgo* spp. using the de Wit et al. 2012 calibration (blue) and the Toyofuku, 2000 calibration (green) compared with the 5-point moving average derived from the three other benthic species.

conditions have to be similar. Unfortunately, this study lacks the data-points required to evaluate the use of *Pyrgo spp.* Mg/Ca as a temperature proxy across the Holocene due to equipment failure.

Another reason for the great differences in Mg incorporation could be inherent to differences in size [Dueñas-Bohórquez et al., 2011]. *Pyrgo spp.* duplicate measurements do not indicate that size differences introduce significant deviations in Mg/Ca incorporation. There does appear to be a positive correlation between test size and Mn incorporation as emphasized by de Wit et al., 2012. Larger *Pyrgo spp.* specimens live deeper infaunal, where they calcify under elevated pore water Mn concentrations. *Pyrgo* species have also been documented to migrate vertically, from living epifaunal on the sediment surface to infaunal to depths of 3 cm [Linke and Lutze, 1993]. Possibly, larger specimens spend more time deeper in the sediment or small individuals calcify faster than large individuals [Sperro and Lea, 1993].

The high scatter in *U. mediterranea* could thus very well be inherent to similar differences in infaunal habitat. This scatter is, however, mainly present in the warmer intervals, although larger specimens exist in both warm and cold intervals. There should thus be another process responsible for the scatter in temperature.

The answer is again likely related to the habitat of the infaunal species. Carbon isotopes extracted from infaunal species have already been found unreliable [Cacho et al., 2006]. This statement is funded on a difference in carbon composition between the pore and bottom water. Both *U. mediterranea* and *Pyrgo spp.* could reflect the Mg/Ca of both pore and bottom water during the both in and epifaunal stages of their life.

Another process which presumably introduces an additional error involving infaunal species is the carbonate ion effect [section 3.2.2]. Pore waters come to rapid equilibration with calcium carbonate in shallow, approximately centimetres, depths within the sediment [Martin et al., 1996; Martin et al., 2006]. However, infaunal benthic foraminifera that calcify only from pore waters below the shallow subsurface zone live at zero  $[CO_3^{2-}]$  are not expected to exhibit carbonate-ion saturation effect [Elderfield et al., 2006]. Nevertheless, it could be that smaller infaunal specimens incorporate a decreased carbonate ion effect which lowers the incorporated Mg/Ca concentration and therefore results in lower temperature estimation. Future Mg/Ca temperature reconstructions should thus select specimens of equal size.

Note that the carbonate ion effect on the epifaunal species is expected to be minimal at the studied site. First, the effect is minimal at temperatures higher than 3 degrees [Elderfield et al., 2006]. Furthermore, under saturated waters mainly exist in the Pacific while Atlantic waters are relatively oversaturated [Rosenthal et al., 1997]. Moreover, relatively high temperature and carbonate ion saturation (149 $\mu$ mol/kg) are documented for the WMDW in the west Alboran Sea, introducing a minimum sensitivity of the analysed Mg/Ca ratios to carbonate saturation [Cacho et al., 2006; Bryan and Marchitto, 2008]. Since the site likely reflects the lower core of MOW, this concentration is expected to be comparable to this site. It is however, not yet clear what effect oversaturated carbonate conditions have on Mg/Ca concentrations [Elderfield et al., 2006]

Another process affecting the applicability of Mg/Ca as a temperature proxy on both species is related to the high salinities of MOW. Higher salinities, however, should theoretically overestimate the extracted Mg/Ca and thereby temperatures [Ferguson et al., 2008] and can thus not explain the positive offset of 5 degrees. The next section briefly evaluates the value of the few presented clumped temperatures.

### 6.2.3 Applicability of the clumped paleothermometer

Although the clumped thermometer should theoretically supply similar temperatures for different species [Eiler, 2007] there is a significant offset between *Pyrgo spp.* and *C. pachyderma* and *U. mediterranea* (*H. elegans* has not yet been measured). Possible sources of uncertainty involving the reconstructed clumped temperatures might be the estimated calcification temperatures, species-specific vital effects, pH variations between the seawater and the vacuole water of the species and possible kinetic effects at temperatures lower than 10°C [Grauel et al., 2013]. Apparently *Pyrgo spp.* is less applicable as a clumped temperature proxy related to some of these factors. Exclusion of the

*Pyrgo spp.* temperature estimates increases both the Holocene and Glacial temperature estimations by 1 degree to respectively 12.4 and 10°C. The remaining offset between glacial Mg/Ca and clumped temperature estimates could still be explained by the doubled deviation in the clumped reconstruction.

Apparently, the measured aliquots are still too little to provide an accurate reconstruction, although *C. pachyderma* and *U. mediterranea* suggest a similar range of temperatures (Appendix II). The state-of-the-art calibration used in this study supposedly works well for benthic species from the Mediterranean [Grauel et al., 2013]. However, at the current state of development it is still necessary to integrate a large number of analyses to detect small-scale temperature changes. The fact that Mg/Ca measurements neither indicate a big temperature gradient between Holocene and Glacial proves this statement.

Summing up, the applied calibrations likely introduce an error within the temperature reconstruction. It is, however, at this point, not possible to quantify the introduced error. The accuracy of the reconstructions potentially increases with calibrations more suitable for the temperature range at the studied site.

Furthermore, epifaunal species provide a more accurate temperature reconstruction than infaunal species due to the carbonate ion effect and differences between pore and bottom water chemistry related to the size of the specimens.

Still, the presented temperature reconstruction (Fig. 16) is the best possible match with the current available calibrations. Moreover, the trend in temperatures across the termination is likely unaffected by the introduced error. In the next section the combination of proxy records is further analysed and discussed.

## 6.2. Evolution of Mediterranean Outflow

In this section the proxy records across the termination are discussed with respect to the evolution of the MOW and circulation in the Gulf of Cadiz. Starting with the transition from the LGM to the Holocene, the section further zooms in on the events revealed across S1 and H1 in order to evaluate the shallow source hypothesis [see chapter 2].

### 6.2.1. Across the termination

#### *Gulf of Cadiz*

Although temperature data reveals no glacial to interglacial trend, stable oxygen isotopes of both planktic and benthic species clearly indicate the last glacial termination. Furthermore both records time well with the GISP2 ice record and LR04 stack. The pronounced drop within both records across the termination is very similar to other records in the Gulf of Cadiz [Voelker et al., 2006, Toucanne et al., 2007].

Also the stable carbon isotopes do not show a great difference between the LGM and the Holocene. Planktic  $\delta^{13}\text{C}$  does seem to be delayed with respect to  $\delta^{18}\text{O}$  in the Holocene. This could imply that surface environments stabilized only ~3 kyr after Greenland ice sheets stabilized. The control of the Greenland ice sheets on the Gulf of Cadiz upper waters is also reflected by the doubled glacial variability in planktic oxygen isotopes as emphasized in other studies [e.g. Mulder et al., 2002; Toucanne et al., 2007 Sierro et al., 2005 Cacho et al., 2006]. The polar front presumably exceeded far further south during the LGM. Millennial DO-like variability could have quickly forced surface water salinity and temperature to drop during melting phases, resulting in a more pronounced variation. This DO-like control on mid latitude environments has also been acknowledged by Cacho et al., 2006.

#### *The Outflow*

Sedimentation has been relatively constant across the termination but was more than doubled across the LGM [section 3.5]. This could imply that the MOW has been stronger across the LGM.

However, magnetic susceptibility measurements indicate that sedimentation increased towards the Holocene.

On the other hand, bottom water reconstructions show that although temperatures are similar, salinity was slightly larger across the LGM. Applying the relationship between  $\delta^{18}\text{O}_{\text{ivf-sw}}$  and salinity established by Pierre, 1999, this slight increase represents an increase in salinity of about 2‰ (Fig. 17). This increase is in agreement with other studies. Even when Mediterranean excess evaporation remained constant at present values during the LGM, the MOW volume would have reduced substantially due to the low sea level consequently enhancing Mediterranean salinity and therefore salinities of the WMDW and LIW [e.g. Rohling and Bryden, 1994].

### 6.2.2. H1, AB and the YD

#### *Gulf of Cadiz*

Almost all records reveal a significant change across H1. It is remarkable that no abundant peaks of cold sinistral *N. pachyderma* have been encountered across the termination. Its morphology in this region is, however, suggested to be much smaller and different than the polar form [Toucanne, comment], which presumably makes it difficult to detect. Toucanne et al., 2007 encountered these polar species in IRD enriched samples and this way pinpointed H1 and YD. This finding supports the hypothesis that icebergs reached middle latitudes across both stadials [Kudrass, 1973]. Clearly the surges have been sufficient to affect the Gibraltar Exchange [Rogerson et al., 2008].

Across H1, a peak in surface  $\delta^{13}\text{C}$  might suggest an increased primary productivity. This increase in productivity can be forced by an increase in upwelling and thus nutrient availability, or increasing nutrient supply from the continent. Seasonal upwelling at present is relatively weak and only occurs in the northernmost Gulf of Cadiz [Schönfeld et al., 2002]. Furthermore, an increase in nutrient input by land should be reflected by an increase in grain size and/or an increase in magnetic susceptibility. The slight increase in ferromagnetic grains at the start of H1 could prove this increase in continental discharge. However, an increase in discharge is likely to further decrease the  $\delta^{13}\text{C}$  of the surface waters due to a generally light terrigenous  $\delta^{13}\text{C}_{\text{DIC}}$ . On the other hand, it could also be that nutrient availability has been higher in the Gulf of Cadiz due to a different circulation during the cold stadials.

Another explanation for an increase in  $\delta^{13}\text{C}$  across H1 might be inherent to the ice surge itself. Freshwater has a far lighter  $\delta^{13}\text{C}$  value than salt water [Akse, comment]. An increase in  $\delta^{13}\text{C}$  with a similar magnitude across the YD evidences this hypothesis. The presented data, however, does not allow a reconstruction of surface water temperatures or an estimation of paleoproductivity. It is, nevertheless, clear that a drastic change in surface water fauna occurred across H1 and the YD. Additional surface productivity proxies could provide new insights into this event.

#### *The Outflow*

Simultaneous with the presumable ice surge in the surface ocean, the deep sea witnessed a drop in temperature simultaneous with a decrease in salinity at the start of H1. This drop in salinity is synchronous with the drop in overturning reconstructed by McManus et al. in 2004 (Fig. 20). There are two possible scenarios that explain the drop in both temperature and salinity.

First, if the path of the lower core was oriented in a similar way as in present times, data indicated that the density and thus the strength of the lower core reduced. Low densities in WMDW dominated the last part of H1 presumably related to the deglacial sea level rise, which enhanced Atlantic inflow and freshened the Mediterranean waters. Sub sequentially freshening of surface waters in the Alboran Sea could have been of such a magnitude that enhanced buoyancy resulted in inhibited deep water overturning during the cold, stadial part of H1. Consequently, the lower/dense core of the MOW in the Gulf of Cadiz reduced during H1 [Cacho et al., 2005, Voelker et al., 2006; Toucanne et al., 2007].

However, if the lower core of the MOW indeed freshened across H1 as observed, it is questioned whether it would still be present at the same depth. It is more likely that WMDW would then overlay the denser NADW. In this scenario, the NADW would be oriented at a depth of 1000 meters. This is expected to be revealed by the benthic  $\delta^{13}\text{C}$ . Additional  $\delta^{13}\text{C}$  measurements on epifaunal benthics could provide insights into this hypothesis. If this hypothesis is true, then at least the lower core of the MOW did not increasingly promote overturning across H1.

Another explanation could be related to a change in the path of the lower core across H1. This hypothesis is also likely since sedimentation rate was reduced at this time [Fig. 11]. However, magnetic susceptibility suggests a slight increase in coarse sedimentation. A reconstruction of the flow path of the MOW across the termination could potentially solve this apparent contradiction.

Across the transition from H1 to A/B, both salinity and temperature increased. This indicates that the lower core again regained its previous LGM strength; WMDW deep water formation presumably restored at this time. An increase in silt sedimentation, however, contradicts this hypothesis. Nevertheless, the silt/clay proxy is very qualitative and small excursions like the one at A/B might also be related to experimental errors. Sophisticated grain size analysis as performed by Voelker et al. in 2006 could improve the qualification of flow strength. The increase in salinity simultaneous with the increased overturning within the AB (Fig. 20) is slightly lower than the salinity across the LGM. If indeed MOW promoted a restart of AMOC across the H1 to AB transition a much higher magnitude of change would have been expected.

Similar to H1, the lower core again appears to reduce across the YD revealed by both a decrease in salinity and temperature. This trend seems to continue across the deposition of S1 in the Eastern Mediterranean. The lower core of the MOW appears to be unable to restore across the transition from YD to S1. Note that the timing of the salinity (and temperature) excursions are quite synchronous with the documented events of both the millennial climate events in the Greenland ice core and the deposition of S1 in the Eastern Mediterranean. Apparently, climate change affected the circulation in the Mediterranean within a period of 1,000 years.

### 6.2.3. S1

Sapropel formation is presumably related to a stagnation of the water column in response to an intensified monsoon [Rossignol-Strick et al., 1982]. At times of S1 deposition, the surface waters of the Gulf of Cadiz remain relatively stable, although the rapid excursion in planktic  $\delta^{18}\text{O}$  could indicate an increase in discharge due to the enhanced monsoon in relation to a precession minimum. If this is true, the effect would, however, be expected to last for a longer period of time.

As expected, deep sea proxies do indicate quite drastic changes. Even the highly variable benthic  $\delta^{13}\text{C}$  shows a significant decrease which tunes perfectly to an extreme increase in silt sedimentation. Furthermore, the decrease in salinity (6‰) is thrice as much as witnessed across H1, associated with a temperature decrease of similar magnitude.

According to de Lange et al., in 2008, the whole eastern Mediterranean basin was predominantly oxygen-free below  $\sim 1.8$  km during basin-wide synchronous S1 formation. It is suggested that LIW formation substantially reduced or stopped during S1 deposition causing a substantial decrease in MOW. In this case, the contribution of the upper core of the MOW at the site might be more important than previously thought. A reduction in LIW could nevertheless also have reduced the formation of WMDW due to lateral entrainment along the deep Mediterranean

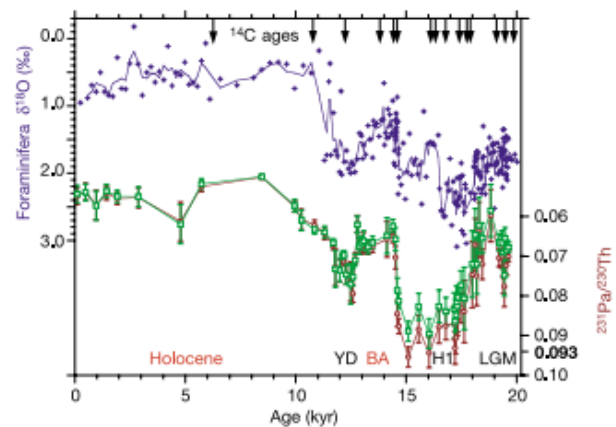


Figure 20: Pa/Th as a proxy for overturning strength. The reduction in overturning across H1 correlates with the reduction in salinity (this study). The increase in overturning after H1 matches the increase in salinity across BA [adapted from McManus et al., 2004]

bathymetry. Still, it is remarkable that the decrease in salinity and temperature starts prior to sapropel formation. This might be explained by the reduced WMDW formation across the YD.

The data nevertheless clearly reveals that not only across H1 and the YD but also across S1 the lower core of MOW either reduced or experienced a deviating flow path. During these times, NADW likely intruded the studied site which could be indicated by the significant shift in benthic  $\delta^{13}\text{C}$ . Now that all records have been interpreted, the shallow source hypothesis is evaluated.

### 6.3. Evaluation of the shallow source hypothesis

Penaud et al., 2011 states that the MOW could be the trigger switching between stadial and interstadial modes of AMOC. The data presented here does not validate this hypothesis.

The presented data, however, primarily reflects changes in the lower core. It might be that the upper core was more intense across the termination or that both cores changed their flow paths. The deep sea salinity record of the Alboran Sea indicates that WMDW reduced across H1 prolonging across the YD (Fig. 21). Moreover, according to Voelker et al., 2006, the WMDW was the major source of MOW during the last glacial.

This does indicate that the lower core indeed decreased in strength across both cold stadials.

Nevertheless, the increased salinity of the MOW during the LGM (+2‰) is expected and stated to have affected the outflow and thus the export of salt to the North Atlantic.

As mentioned in chapter 2, across the cold LGM, the sea level was 120 meters lower than today [Fairbanks, 1989] lowering the exchange of water through the strait of Gibraltar. Combined with a high buoyancy loss in the northwest Mediterranean [Hayes et al., 2005; Kuhlemann et al., 2008] deep water in the Mediterranean substantially increased in salinity [Rogerson et al., 2005]. At these times the MOW settled at a much greater depth than today [Rogerson et al., 2006; Voelker et al., 2006]. Proxy data implies that the plume even reached down to about 2,600m during H1 [Skinner and Elderfield, 2007]. The inferred salt discharge into the North Atlantic in response to the sea level increase from 17.5 to 14.5 ka B.P. would have provided an important preconditioning for abrupt resumption of intermediate and deep overturning around 14.6 ka [Gherardi et al., 2005]. Moreover, the abrupt shoaling of the MOW plume to its present depth range around 15.0-14.5 ka B.P. would likely have reversed the potential density relationship between Glacial North Atlantic and Antarctic Intermediate Waters, which is considered critical for a resumption of MOC [Rickaby and Elderfield, 2005].

The clear contradiction with the presented data might again be explained by the upper core of the MOW. It might be that the upper core of the MOW increased in strength after H1 [Voelker et al., 2006]. According to Voelker et al., 2006, a southward intrusion of subtropical gyre in response to southward movement of the polar front during H1 resulted in input of saline water into the Mediterranean, which removed the freshwater cap in response to H1. This resulted in a restart of WMDW formation. Subsequently a stronger MOW left the Mediterranean Sea and delivered its low buoyancy water to the north restoring the AMOC across the termination. Higher salinity measured at this time in the North Atlantic evidences this hypothesis [Rickaby and Elderfield, 2005].

A similar approach as performed in this study but then involving the lower core of the MOW across the same interval might shed new light on these contradictions and thus on the control of MOW on overturning. It is nevertheless clear that the cause of MOW variability is inherent to both

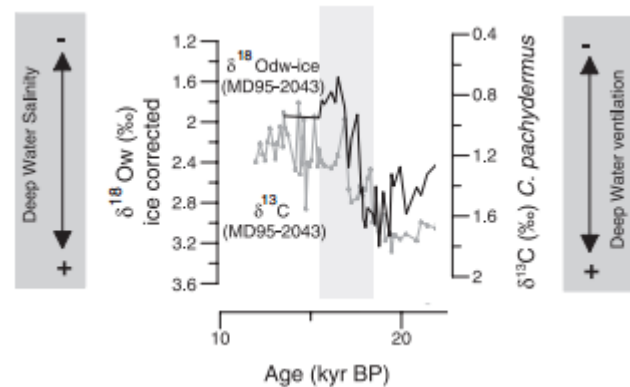


Figure 21: Deep water salinity and ventilation in the western Alboran Sea indicating a decrease in salinity induced by a decrease in deep water formation across H1 (grey interval) [adapted from Cacho et al., 2005]



the sea level of the Strait of Gibraltar and the extent of deep water formation in the Mediterranean Sea.

The presented data does not indicate that MOW increased over the termination and acted as a salt source to reinitiate the AMOC. Whether or not the upper core acted as the responsible feedback mechanism remains unresolved. Other oceanic feedbacks could be more important. For instance it might be more likely that salty waters accumulated in the Caribbean during cold periods could reach the North Atlantic during the termination [see chapter 2].

## 6.4. Outlook

The previous section emphasizes that further research should find a way to infer changes in both the upper and the lower core of outflow. It should also aim to reconstruct the flow path of the MOW across glacial to interglacial transitions. Furthermore independent surface proxies are needed to infer the influence of the Iberian deltas at the site. This way quantitative reconstructions of past flow dynamics in the Gulf of Cadiz become available. It might then even be possible to initiate a model study in the Gulf of Cadiz to see what happens to the bathymetry across glacial to interglacial transitions. Inspired by Schönfeld, 1997, one could even try to gain insights into the flow dynamics based on a reconstruction of the benthic community.

Regarding the applicability of both the clumped and the Mg/Ca paleothermometer, additional clumped measurements across S1 and H1 are underway. These could provide additional proof for the negative excursions in temperature revealed by the Mg/Ca estimates and could provide insights into the applicability of the proxy as a temperature indicator.

Unfortunately, Mg/Ca calibrations are still subject to much uncertainty. Improving the calibrations and identifying and solving the offset in temperatures should be a primary aim in further studies. These studies should mainly focus on epibenthic species of similar size. Moreover, Sr/Ca should be measured in order to gain a secondary estimation of contamination levels. Filling in the gaps in the temperature reconstructions with additional *H. elegans* specimens could provide insight into the best applicable benthic species.

In relation to the outflow, insights into surface circulation in the Gulf of Cadiz are also helpful. Valuable additional analysis for this area could be surface temperature productivity and temperature reconstructions in order to validate freshwater input during stadials and in order to better reveal DO-cyclicity.

## 7. Conclusion

This study aimed to reconstruct the hydrographic properties of the Mediterranean Outflow across the last glacial termination in order to validate the proposed control of the MOW on restarting AMOC across stadial to interstadial transitions.

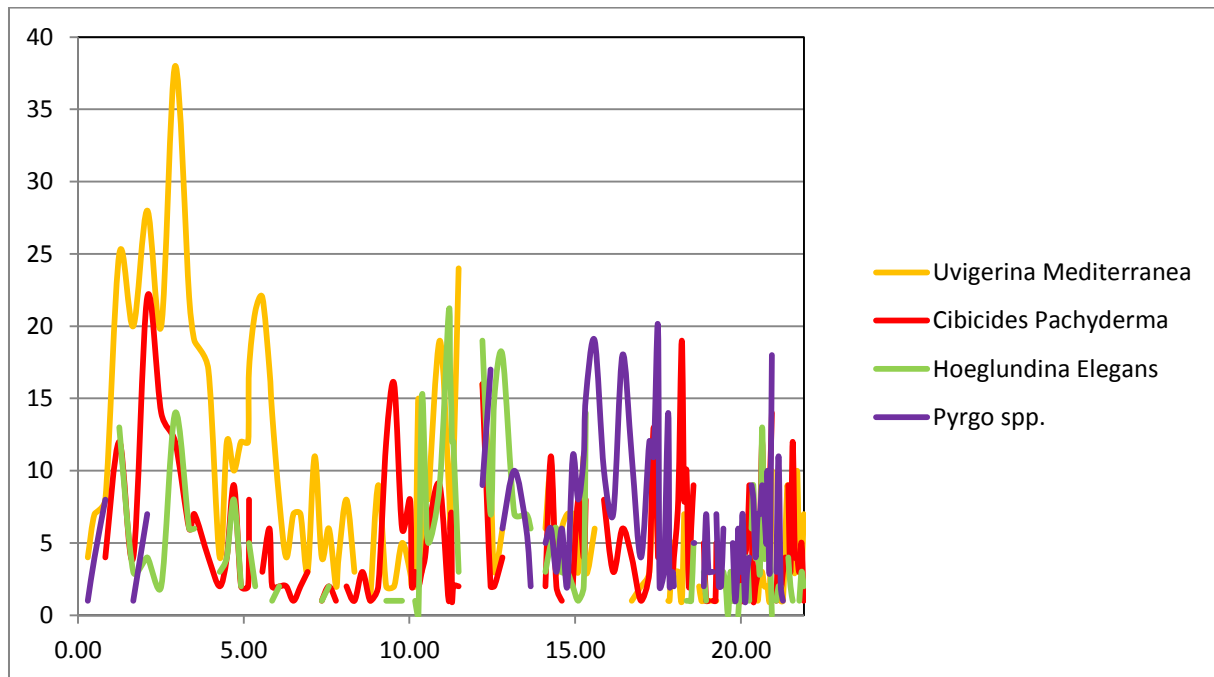
Reconstructed bottom water temperature and salinity do not indicate that the lower core of the MOW has promoted overturning across the last termination. It is more likely that the lower core repeatedly reduced or even shut down. Furthermore, the lower core is concluded to be relatively stable during glacial and interglacial times. Data suggests a reduction of the lower core across H1 and YD due to intrusion of the freshwater surges into the Gulf of Cadiz and the Alboran Sea. The presumably shutdown of the lower core across S1 is likely induced by stagnation of the water column in the Eastern Mediterranean.

Although salinities at the studied site are slightly higher across the LGM (+2‰) the increase in density of the lower MOW core after sea level rise across H1 was not substantial enough to promote overturning. Further studies can validate these conclusions through a reconstruction of both the upper and lower core across the termination. An increase in sea level in response to the glacial termination might have predominately increased the strength of the upper core. Further studies should also aim on reconstructing the flow path of the MOW across the transition. Moreover, the influence of the Iberian river systems on sedimentation in the Gulf of Cadiz has to be better constrained.

Regarding the applicability of the temperature proxies it is first concluded that both the Mg/Ca and the clumped paleothermometer still incorporate significant error margins which hamper the bottom water salinity estimation. In view of the Mg/Ca applicability, the 5 degrees offset might be prevented by using only epifaunal benthics and specimens of similar size. Moreover core-top calibrations or culture calibrations with a similar set of environmental parameters should increase the accuracy of the measurements.

In view of the clumped paleothermometry there appears to be an unexpected offset between different benthics. Culture calibrations could highlight the origin of this offset. At the moment, the standard deviation still prevents an accurate reconstruction.

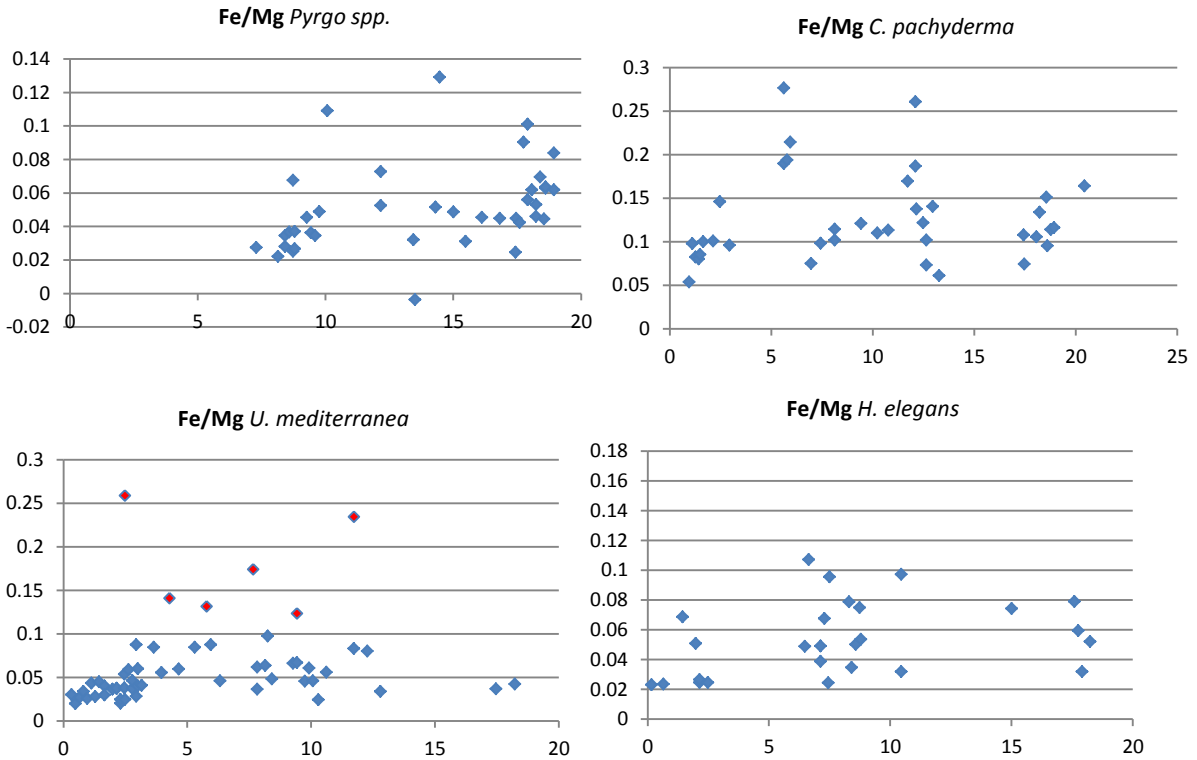
## Appendices



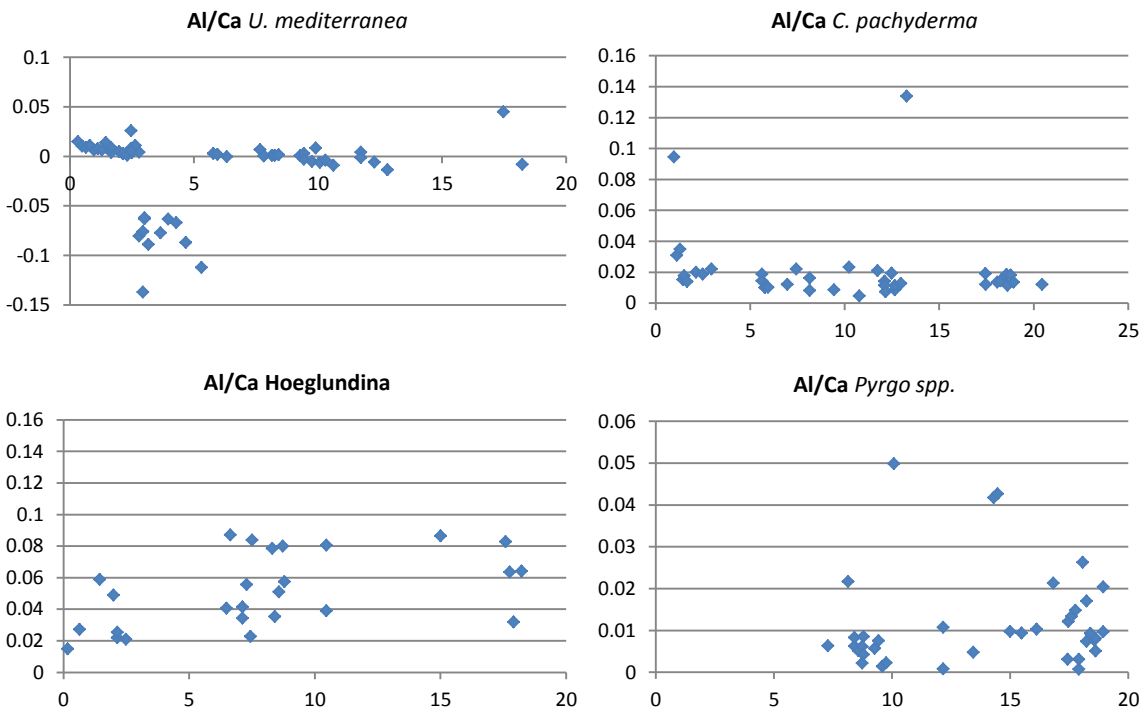
Appendix I: Benthic abundances: yellow: *U. mediterranea*, red: *C. pachyderma*, green: *H. elegans*, purple: *Pyrgo spp.*

Mg/Ca	AVG	STD	Samples	Clumped	AVG	STD	Aliquots
Holocene	8.3	2.6	32	Holocene	8.8	5.5	30
S1	4.2	2.6	11	S1	6.7	4.5	11
YD	4.3	0.9	3	YD	x	x	x
A/B	7.2	2.5	9	A/B	x	x	x
H1	3.2	1.0	8	H1	9.2	3.8	6
Glacial	6.7	1.7	21	Glacial	11.4	5.6	19

Appendix II: Paleo-temperatures (average and standard deviation) of six time slices across the last termination. Mg/Ca is measured on samples of 300 $\mu$ g and clumped isotopic composition on aliquots of 200  $\mu$ g



Appendix III: Fe/Mg values from analysed species. These figures include values (red) that have been removed from BWT reconstructions. Negative values are caused by errors with blanks.



Appendix IV: Al/Ca values from analysed species. Similar to Fe/Mg these plots contain values removed prior to BWT reconstruction. The negative values for Al/Ca in *U. mediterranea* are also caused by blanco induced errors.

## References

- Aagaard, K. (1981). On the deep circulation in the Arctic Ocean. *Deep Sea Research Part A. Oceanographic Research Papers*, 28(3), 251-268.
- Ahn, J., and Brook, E. J. (2008). Atmospheric CO<sub>2</sub> and climate on millennial time scales during the last glacial period. *Science*, 322(5898), 83-85.
- Alley, R. B., & Clark, P. U. (1999). The deglaciation of the northern hemisphere: a global perspective. *Annual Review of Earth and Planetary Science*, 27, 149-182.
- Marshall, S. J., Hillaire-Marcel, C., Bilodeau, G., & Veiga-Pires, C. (1999). A glaciological perspective on Heinrich events. *Mechanisms of global climate change at millennial time scales*, 243-262.
- Ambar, I., and Howe, M. R. (1979). Observations of the Mediterranean outflow—II The deep circulation in the vicinity of the Gulf of Cadiz. *Deep Sea Research Part A. Oceanographic Research Papers*, 26(5), 555-568.
- Ambar, I., Serra, N., Brogueira, M. J., Cabeçadas, G., Abrantes, F., Freitas, P., ... and Gonzalez, N. (2002). Physical, chemical and sedimentological aspects of the Mediterranean outflow off Iberia. *Deep Sea Research Part II: Topical Studies in Oceanography*, 49(19), 4163-4177.
- Anderson, R. F., Ali, S., Bradtmiller, L. I., Nielsen, S. H. H., Fleisher, M. Q., Anderson, B. E., and Burckle, L. H. (2009). Wind-driven upwelling in the Southern Ocean and the deglacial rise in atmospheric CO<sub>2</sub>. *Science*, 323(5920), 1443-1448.
- Astraldi, M., Gasparini, G. P., Vetrano, A., and Vignudelli, S. (2002). Hydrographic characteristics and interannual variability of water masses in the central Mediterranean: a sensitivity test for long-term changes in the Mediterranean Sea. *Deep Sea Research Part I: Oceanographic Research Papers*, 49(4), 661-680.
- Barker, S., Greaves, M., and Elderfield, H. (2003). A study of cleaning procedures used for foraminiferal Mg/Ca paleothermometry. *Geochemistry, Geophysics, Geosystems*, 4(9).
- Baringer, M. O. N., and Price, J. F. (1997). Mixing and spreading of the Mediterranean outflow. *Journal of Physical Oceanography*, 27(8), 1654-1677.
- Berger, A., & Loutre, M. F. (1991). Insolation values for the climate of the last 10 million years. *Quaternary Science Reviews*, 10(4), 297-317.
- Bernasconi, S. M., Schmid, T. W., Grauel, A. L., & Mutterlose, J. (2011). Clumped-isotope geochemistry of carbonates: a new tool for the reconstruction of temperature and oxygen isotope composition of seawater. *Applied Geochemistry*, 26, S279-S280.
- Bigg, G. R., & Wadley, M. R. (2001). Millennial-scale variability in the oceans: An ocean modelling view. *Journal of Quaternary Science*, 16(4), 309-319.
- Bigg, G. R. (2003). *The oceans and climate*. Cambridge University Press.
- Bintanja, R., and Van de Wal, R. S. W. (2008). North American ice-sheet dynamics and the onset of 100,000-year glacial cycles. *Nature*, 454(7206), 869-872.
- Bond, G., Broecker, W. S., Johnsen, S., McManus, J., Labeyrie, L., Jouzel, J., & Bonani, G. (1993). Correlations between climate records from North Atlantic sediments and Greenland ice. *Nature*, 365(6442), 143-147. *Earth and Planetary Science Letters*, 112, 149-182.
- Bond, G. C., Showers, W., Elliot, M., Evans, M., Lotti, R., Hajdas, S., Johnson, S. (1999). The North Atlantic's 1-2 kyr climate rhythm: relation to Heinrich events, Dansgaard/Oeschger cycles and the little ice age. *Geophysical Monograph Series*, 112, 35-58.
- Bower, A. S., Serra, N., & Ambar, I. (2002). Structure of the Mediterranean Undercurrent and Mediterranean Water spreading around the southwestern Iberian Peninsula. *Journal of Geophysical Research: Oceans* (1978–2012), 107(C10), 25-1.
- Boyle, E. A. (2000). Is ocean thermohaline circulation linked to abrupt stadial/interstadial transitions?. *Quaternary Science Reviews*, 19(1), 255-272.
- Broecker, W. S., Peng, T. H., and Beng, Z. (1982). *Tracers in the Sea*. Lamont-Doherty Geological Observatory, Columbia University.
- Broecker, W. S., Massive iceberg discharges as triggers for global climate change, *Nature*, 372, 421-424, 1994.
- Brown, S. J., and Elderfield, H. (1996). Variations in Mg/Ca and Sr/Ca ratios of planktic foraminifera caused by postdepositional dissolution: Evidence of shallow Mg-dependent dissolution. *Paleoceanography*, 11(5), 543-551.
- Bryan, S. P., and Marchitto, T. M. (2008). Mg/Ca-temperature proxy in benthic foraminifera: New calibrations from the Florida Straits and a hypothesis regarding Mg/Li. *Paleoceanography*, 23(2).
- Bryden, H. L., and Stommel, H. M. (1984). Limiting processes that determine basic features of the circulation in the Mediterranean-sea. *Oceanologica Acta*, 7(3), 289-296.
- Bryden, H. L., Longworth, H. R., & Cunningham, S. A. (2005). Slowing of the Atlantic meridional overturning circulation at 25°N. *Nature*, 438(7068), 655-657.
- Candela, J. (2001). 7 Mediterranean water and global circulation. *International Geophysics*, 77, 419-XLVIII.
- Chan, W. L., & Motoi, T. (2003). Effects of stopping the Mediterranean outflow on the southern polar region. *Polar Meteorology and Glaciology*, 17, 25-35.
- Cappelli, E. L. G., Holbourn, A., Kuhnt, W., Regenber, M., A new benthic Mg/Ca temperature calibration to reconstruct thermocline temperature variability Cronin, Thomas M. (1999). *Principles of Climatology*. New York: Columbia University Press. p. 204. ISBN 0-231-10955-5. in the Indonesian archipelago. Institute of Geosciences, Christian-Albrechts-University, Kiel, Germany (unpublished)
- Chapman, J. A., and Wilson, R. C. L. (2005). *The great Ice Age: climate change and life*. Routledge.
- Church, J. A. and N.J. White (2006), A 20th century acceleration in global sea level rise, *Geophysical Research Letters*, 33
- Clark, P. U., Alley, R. B., and Pollard, D. (1999). Northern Hemisphere ice-sheet influences on global climate change. *Science*, 286(5442), 1104-1111.
- Clark, P. U., Pisias, N. G., Stocker, T. F., & Weaver, A. J. (2002). The role of the thermohaline circulation in abrupt climate change. *Nature*, 415(6874), 863-869.

- Cook, C. P., T. van de Flierdt, T. Williams, Sidney R. Hemming, M. Iwai, M. Kobayashi, F. J. Jimenez-Espejo, C. Escutia, J. González, B. Khim, R. McKay, S. Passchier, L. Tauxe, S. Sugisaki, A. L. Galindo, M. O. Patterson, S. M. Bohaty, C. R. Riesselman, F. Sangiorgi, E. Pierce, H. Brinkhuis, and IODP Expedition 318 Scientists. Dynamic Behaviour of the East Antarctic Ice Sheet during Pliocene Warmth, *Nature Geoscience*, July 2013
- Criado-Aldeanueva, F., García-Lafuente, J., Vargas, J. M., Del Río, J., Vázquez, A., Reul, A., and Sánchez, A. (2006). Distribution and circulation of water masses in the Gulf of Cadiz from in situ observations. *Deep Sea Research Part II: Topical Studies in Oceanography*, 53(11), 1144-1160.
- Cubasch, U., Meehl, G. A., Boer, G. J., Stouffer, R. J., Dix, M., Noda, A., ... & Yap, K. S. (2001). Projections of future climate change. , in: JT Houghton, Y. Ding, DJ Griggs, M. Noguer, PJ Van der Linden, X. Dai, K. Maskell, and CA Johnson (eds.): *Climate Change 2001: The Scientific Basis: Contribution of Working Group I to the Third Assessment Report of the Intergovernmental Panel*, 526-582.
- Dansgaard, W., Johnsen, S. J., Clausen, H. B., Dahl-Jensen, D., Gundestrup, N. S., Hammer, C. U., ... and Bond, G. (1993). Evidence for general instability of past climate from a 250-kyr ice-core record. *Nature*, 364(6434), 218-220.
- De Lange, G. J., Thomson, J., Reitz, A., Slomp, C. P., Principato, M. S., Erba, E., and Corselli, C. (2008). Synchronous basin-wide formation and redox-controlled preservation of a Mediterranean sapropel. *Nature Geoscience*, 1(9), 606-610.
- Denton, G. H., Anderson, R. F., Toggweiler, J. R., Edwards, R. L., Schaefer, J. M., & Putnam, A. E. (2010). The last glacial termination. *Science*, 328(5986), 1652-1656.
- Dueñas-Bohórquez, A., Raitzsch, M., de Nooijer, L. J., and Reichart, G. J. (2011). Independent impacts of calcium and carbonate ion concentration on Mg and Sr incorporation in cultured benthic foraminifera. *Marine Micropaleontology*, 81(3), 122-130.
- Epstein, S., Buchsbaum, R., Lowenstam, H. A., and Urey, H. C. (1953). Revised carbonate-water isotopic temperature scale. *Geological Society of America Bulletin*, 64(11), 1315-1326.
- Ewen, T. L., A. J. Weaver, and A. Schmittner (2004), Modelling carbon cycle feedbacks during abrupt climate change, *Quat. Sci. Rev.*, 23(3 – 4), 431 – 448.
- Fairbanks, R. G. (1989). A 17, 000-year glacio-eustatic sea level record: influence of glacial melting rates on the Younger Dryas event and deep-ocean circulation. *Nature*, 342(6250), 637-642.
- Faugères, J. C., Gonthier, E., and Stow, D. A. (1984). Contourite drift molded by deep Mediterranean outflow. *Geology*, 12(5), 296-300.
- Ferguson, J. E., Henderson, G. M., Kucera, M., and Rickaby, R. E. M. (2008). Systematic change of foraminiferal Mg/Ca ratios across a strong salinity gradient. *Earth and Planetary Science Letters*, 265(1), 153-166.
- Ganachaud, A., Wunsch, C. (2000) Improved estimates of global ocean circulation, heat transport and mixing from hydrographic data. *Nature* 408:453–457
- García Lafuente, J., Sánchez Román, A., Díaz del Río, G., Sannino, G., and Sánchez Garrido, J. C. (2007). Recent observations of seasonal variability of the Mediterranean outflow in the Strait of Gibraltar. *Journal of Geophysical Research: Oceans* (1978–2012), 112(C10).
- Garrels, R. M., Mackenzie, F. T., and Maynard, J. B. (1988). *Chemical Cycles in the Evolution of the Earth*. New York: Wiley.
- Gelderloos, R., Katsman, C. A., & Drijfhout, S. S. (2011). Assessing the roles of three eddy types in restratifying the Labrador Sea after deep convection. *Journal of Physical Oceanography*, 41(11), 2102-2119.
- Gregory, J., Dixon, K., Stouffer, R., Weaver, A., Driesschaert, E., Eby, M., Fichetef, T., Hasumi, H., Hu, A., Jungclaus, J., Kamenkovich, I., Levermann, A., Montoya, M., Murakami, S., Nawrath, S., Oka, A., Sokolov, A., Thorpe, R. (2005) A model intercomparison of changes in the Atlantic thermohaline circulation in response to increasing atmospheric CO2 concentration. *Geophys. Res. Lett* 32:L12703.1–L12703.5
- Groote, P.M., Stuiver, M., White, J. W. C., Johnsen, S. & Jouzel, J. Comparison of oxygen isotope records from the GISP2 and GRIP Greenland ice cores. *Nature* 366, 552-554 (1993).
- Grauel, A. L., Schmid, T. W., Hu, B., Bergami, C., Capotondi, L., Zhou, L., & Bernasconi, S. M. (2013). Calibration and application of the 'clumped isotope' thermometer to foraminifera for high-resolution climate reconstructions. *Geochimica et Cosmochimica Acta*, 108, 125-140.
- Hagood, E. L., Kenyon, N. H., Masson, D. G., Akhmetzhanov, A., Weaver, P. P., Gardner, J., and Mulder, T. (2003). Deep-water sediment wave fields, bottom current sand channels and gravity flow channel-lobe systems: Gulf of Cadiz, NE Atlantic. *Sedimentology*, 50(3), 483-510.
- Hagelberg, T. K., Bond, G., and Demenocal, P. (1994). Milankovitch band forcing of sub-Milankovitch climate variability during the Pleistocene. *Paleoceanography*, 9(4), 545-558.
- Haynes, R., and Barton, E. D. (1990). A poleward flow along the Atlantic coast of the Iberian Peninsula. *Journal of Geophysical Research: Oceans* (1978–2012), 95(C7), 11425-11441.
- Hayes, A., Kucera, M., Kallel, N., Saffi, L., & Rohling, E. J. (2005). Glacial Mediterranean sea surface temperatures based on planktonic foraminiferal assemblages. *Quaternary Science Reviews*, 24(7), 999-1016.
- Hays, J. D., Imbrie, J., & Shackleton, N. J. (1976, December). Variations in the Earth's orbit: Pacemaker of the ice ages. *American Association for the Advancement of Science*.
- Heinrich, H. (1988). Origin and consequences of cyclic ice rafting in the northeast Atlantic Ocean during the past 130,000 years. *Quaternary research*, 29(2), 142-152.
- Hemming, S. R. (2004). Heinrich events: Massive late Pleistocene detritus layers of the North Atlantic and their global climate imprint. *Reviews of Geophysics*, 42(1).
- Hewitt, C. D., & Mitchell, J. F. B. (1997). Radiative forcing and response of a GCM to ice age boundary conditions: cloud feedback and climate sensitivity. *Climate Dynamics*, 13(11), 821-834.
- Hill, A. E., & Mitchelson-Jacob, E. G. (1993). Observations of a poleward-flowing saline core on the continental slope west of Scotland. *Deep Sea Research Part I: Oceanographic Research Papers*, 40(7), 1521-1527.

- Imbrie, J., Hays, J. D., Martinson, D. G., McIntyre, A., Mix, A. C., Morley, J. J., ... & Shackleton, N. J. (1984). The orbital theory of Pleistocene climate: Support from a revised chronology of the marine  $\delta^{18}O$  record. In *Milankovitch and climate: Understanding the response to astronomical forcing* (Vol. 1, p. 269).
- Imbrie, J., Boyle, E. A., Clemens, S. C., Duffy, A., Howard, W. R., Kukla, G., ... & Toggweiler, J. R. (1992). On the structure and origin of major glacial cycles 1. Linear responses to Milankovitch forcing. *Paleoceanography*, 7(6), 701-738.
- Imbrie, J., Mix, A. C., & Martinson, D. G. (1993). Milankovitch theory viewed from Devils Hole. *Nature*, 363(6429), 531-533.
- Iorga, M. C., & Lozier, M. S. (1999). Signatures of the Mediterranean outflow from a North Atlantic climatology: 1. Salinity and density fields. *Journal of Geophysical Research: Oceans* (1978–2012), 104(C11), 25985-26009.
- Ivanovic, R. F., Valdes, P. J., Gregoire, L., Flecker, R., & Gutjahr, M. (2014). Sensitivity of modern climate to the presence, strength and salinity of Mediterranean-Atlantic exchange in a global general circulation model. *Climate Dynamics*, 42(3-4), 859-877.
- Jansen, E., Sjøholm, J., Bleil, U., & Erichsen, J. A. (1990). Neogene and Pleistocene glaciations in the Northern Hemisphere and late Miocene—Pliocene global ice volume fluctuations: Evidence from the Norwegian Sea. In *Geological History of the Polar Oceans: Arctic versus Antarctic* (pp. 677-705). Springer Netherlands.
- Jansen, E., & Sjøholm, J. (1991). Reconstruction of glaciation over the past 6 Myr from ice-borne deposits in the Norwegian Sea. *Nature*, 349(6310), 600-603.
- Joos, F., G. K. Plattner, T. F. Stocker, O. Marchal, and A. Schmittner (1999), Global warming and marine carbon cycle feedbacks on future atmospheric CO<sub>2</sub>. *Science*, 284(5413), 464 – 467.
- Katz, M. E., Cramer, B. S., Franzese, A., Hönlisch, B., Miller, K. G., Rosenthal, Y., & Wright, J. D. (2010). Traditional and emerging geochemical proxies in foraminifera. *The Journal of Foraminiferal Research*, 40(2), 165-192.
- Kinder, T. H., and Bryden, H. L. (1987). The 1985–1986 Gibraltar Experiment: Data collection and preliminary results. *Eos, Transactions American Geophysical Union*, 68(40), 786-794.
- Kinder, T. H., and Parrilla, G. (1987). Yes, some of the Mediterranean outflow does come from great depth. *Journal of Geophysical Research: Oceans* (1978–2012), 92(C3), 2901-2906.
- Knorr, G., & Lohmann, G. (2003). Southern Ocean origin for the resumption of Atlantic thermohaline circulation during deglaciation. *Nature*, 424(6948), 532-536.
- Knutti, R., Flückiger, J., Stocker, T., Timmermann, A. (2004) Strong hemispheric coupling of glacial climate through freshwater discharge and ocean circulation. *Nature* 430:851–856
- Kuhlbrodt, T., Griesel, A., Montoya, M., Levermann, A., Hofmann, M., & Rahmstorf, S. (2007). On the driving processes of the Atlantic meridional overturning circulation. *Reviews of Geophysics*, 45(2). Kuhlmann, J., Rohling, E. J., Krumrei, I., Kubik, P., Ivy-Ochs, S., & Kucera, M. (2008). Regional synthesis of Mediterranean atmospheric circulation during the Last Glacial Maximum. *Science*, 321(5894), 1338-1340.
- Laskar, J. (1990). The chaotic motion of the solar system: A numerical estimate of the size of the chaotic zones. *Icarus*, 88(2), 266-291.
- Laskar, J., Joutel, F., and Boudin, F. (1993). Orbital, precessional, and insolation quantities for the Earth from -20 Myr to + 10 Myr. *Astronomy and Astrophysics*, 270, 522-533.
- Lea, D. W., Pak, D. K., & Spero, H. J. (2000). Climate impact of late Quaternary equatorial Pacific sea surface temperature variations. *Science*, 289(5485), 1719-1724.
- Linke, P., and Lutze, G. F. (1993). Microhabitat preferences of benthic foraminifera—a static concept or a dynamic adaptation to optimize food acquisition?. *Marine Micropaleontology*, 20(3), 215-234.
- Locarnini, R. A., O'Brien, T. D., Garcia, H. E., Antonov, J. I., Boyer, T. P., Conkright, M. E., and Stephens, C. (2002). *World Ocean Atlas 2001. Volume 3, Oxygen*.
- MacAyeal, D. R. (1993). Binge/purge oscillations of the Laurentide ice sheet as a cause of the North Atlantic's Heinrich events. *Paleoceanography*, 8(6), 775-784.
- Maier-Reimer, E., U. Mikolajewicz, and A. Winguth (1996), Future ocean uptake of CO<sub>2</sub>: Interaction between ocean circulation and biology, *Clim. Dyn.*, 12(10), 711 – 721.
- Manabe, S., & Stouffer, R. J. (1994). Multiple-century response of a coupled ocean-atmosphere model to an increase of atmospheric carbon dioxide. *Journal of climate*, 7(1), 5-23.
- Manabe, S., and Stouffer, R. J. (1995). Simulation of abrupt climate change induced by freshwater input to the North Atlantic Ocean. *Nature*, 378(6553), 165-167.
- Marchal, O., T.F. Stocker, and F. Joos (1998), Impact of oceanic reorganizations of the ocean carbon cycle and atmospheric carbon dioxide content, *Paleoceanography*, 13(3), 225-244.
- Marchitto, T. M., Lynch-Stieglitz, J., and Hemming, S. R. (2005). Deep Pacific CaCO<sub>3</sub> compensation and glacial–interglacial atmospheric CO<sub>2</sub>. *Earth and Planetary Science Letters*, 231(3-4), 317-336.
- Marshall, J., & Schott, F. (1999). Open-ocean convection: Observations, theory, and models. *Reviews of Geophysics*, 37(1), 1-64.
- Martin, W. R., & Sayles, F. L. (1996). CaCO<sub>3</sub> dissolution in sediments of the Ceara Rise, western equatorial Atlantic. *Geochimica et Cosmochimica Acta*, 60, 243-263.
- Martin, W. R., and Sayles, F. L. (2006). Organic matter oxidation in deep-sea sediments: distribution in the sediment column and implications for calcite dissolution. *Deep Sea Research Part II: Topical Studies in Oceanography*, 53(5), 771-792. Chicago
- Martin, W., Baross, J., Kelley, D., and Russell, M. J. (2008). Hydrothermal vents and the origin of life. *Nature Reviews Microbiology*, 6(11), 805-814.
- Maslin, M. A., Li, X. S., Loutre, M. F., & Berger, A. (1998). The contribution of orbital forcing to the progressive intensification of Northern Hemisphere glaciation. *Quaternary Science Reviews*, 17(4), 411-426.
- Maslin, M., Seidov, D., & Lowe, J. (2001). Synthesis of the nature and causes of rapid climate transitions during the Quaternary. *The Oceans and Rapid Climate Change: Past, Present, and Future*, 9-52.
- Matear, R., and A. Hirst (1999), Climate change feedback on the future oceanic CO<sub>2</sub> uptake, *Tellus*, 51B, 722 – 733.
- Mauritzen, C., Morel, Y., & Paillet, J. (2001). On the influence of Mediterranean water on the central waters of the North Atlantic Ocean. *Deep Sea Research Part I: Oceanographic Research Papers*, 48(2), 347-381.

McCartney, M. S., and Talley, L. D. (1982). The subpolar mode water of the North Atlantic Ocean. *Journal of Physical Oceanography*, 12(11), 1169-1188.

McCartney, M. S., & Mauritzen, C. (2001). On the origin of the warm inflow to the Nordic Seas. *Progress in Oceanography*, 51(1), 125-214.

McCorkle, D. C., Martin, P. A., Lea, D. W., and Klinkhammer, G. P. (1995). Evidence of a dissolution effect on benthic foraminiferal shell chemistry:  $\delta^{13}C$ , Cd/Ca, Ba/Ca, and Sr/Ca results from the Ontong Java Plateau. *Paleoceanography*, 10(4), 699-714.

McManus, J. F., Francois, R., Gherardi, J. M., Keigwin, L. D., & Brown-Leger, S. (2004). Collapse and rapid resumption of Atlantic meridional circulation linked to deglacial climate changes. *Nature*, 428(6985), 834-837.

Milankovitch, Milutin. *Kanon der Erdebestrahlung und seine anwendung auf das eiszeitenproblem*. Königlich Serbische Akademie, 1941.

Mulder, T., Lecroart, T. P., Voisset, M., Schönfeld, J., Le Drezen, E., Gonthier, E., ... and Gervais, A. (2002). Past deep-ocean circulation and the paleoclimate record-Gulf of Cadiz. *EOS, Transactions American Geophysical Union*, 83(43), 481-488.

Mulder, T., Voisset, M., Lecroart, P., Le Drezen, E., Gonthier, E., Hanquiez, V., ... and Morel, J. (2003). The Gulf of Cadiz: an unstable giant contouritic levee. *Geo-Marine Letters*, 23(1), 7-18.

Munk, W., & Wunsch, C. (1998). Abyssal recipes II: energetics of tidal and wind mixing. *Deep-Sea Research Part I*, 45(12), 1977-2010.

New, A. L., Barnard, S., Herrmann, P., & Molines, J. M. (2001). On the origin and pathway of the saline inflow to the Nordic Seas: insights from models. *Progress in Oceanography*, 48(2), 255-287.

Nisancioglu, K. H., Raymo, M. E., & Stone, P. H. (2003). Reorganization of Miocene deep water circulation in response to the shoaling of the Central American Seaway. *Paleoceanography*, 18(1).

Ní Fhlaithearta, S., Reichert, G. J., Jorissen, F. J., Fontanier, C., Rohling, E. J., Thomson, J., and de Lange, G. J. (2010). Reconstructing the sea floor environment during sapropel formation using trace metals and sediment composition. *Paleoceanography*, 25(4).

Nurnberg, D. I. R. K. (1996). Magnesium in tests of *Neogloboquadrina pachyderma* sinistral from high northern and southern latitudes. *Oceanographic Literature Review*, 43(7).

Obata, A. (2007). Climate – carbon cycle response to freshwater discharge into the North Atlantic. *J. Clim.*, 20, 5962 – 5976.

Orr, J. C., Fabry, V. J., Aumont, O., Bopp, L., Doney, S. C., Feely, R. A., ... and Yool, A. (2005). Anthropogenic ocean acidification over the twenty-first century and its impact on calcifying organisms. *Nature*, 437(7059), 681-686.

Pearson, P. N., Ditchfield, P. W., Singano, J., Harcourt-Brown, K. G., Nicholas, C. J., Olsson, R. K., ... and Hall, M. A. (2001). Warm tropical sea surface temperatures in the Late Cretaceous and Eocene epochs. *Nature*, 413(6855), 481-487.

Peliz, Á., Dubert, J., Santos, A. M. P., Oliveira, P. B., and Le Cann, B. (2005). Winter upper ocean circulation in the Western Iberian Basin— Fronts, Eddies and Poleward Flows: an overview. *Deep sea research Part I: Oceanographic research papers*, 52(4), 621-646.

Pénaud, A., Eynaud, F., Sánchez-Goñi, M., Malaizé, B., Turon, J. L., & Rossignol, L. (2011). Contrasting sea-surface responses between the western Mediterranean Sea and eastern subtropical latitudes of the North Atlantic during abrupt climatic events of MIS 3. *Marine Micropaleontology*, 80(1), 1-17.

Petoukhov, V., Claussen, M., Berger, A., Crucifix, M., Eby, M., Eliseev, A. V., ... & Weaver, A. J. (2005). EMIC Intercomparison Project (EMIP–CO2): comparative analysis of EMIC simulations of climate, and of equilibrium and transient responses to atmospheric CO2 doubling. *Climate Dynamics*, 25(4), 363-385.

Pierre, C. (1999). The oxygen and carbon isotope distribution in the Mediterranean water masses. *Marine Geology*, 153(1), 41-55.

Plattner, G.K., F. Joos, T.F. Stocker, and O. Marchal (2001), Feedback mechanisms and sensitivities of ocean carbon uptake under global warming, *Tellus Ser. B-chem. Phys. Meteorol.*, 53(5), 564-592.

Rahmstorf, S. (1994). Rapid climate transitions in a coupled ocean-atmosphere model. *Nature*, 372(6501), 82-85.

Rahmstorf, S. (1998). Influence of Mediterranean outflow on climate. *Eos, Transactions American Geophysical Union*, 79(24), 281-282.

Rahmstorf, S., & Ganopolski, A. (1999). Long-term global warming scenarios computed with an efficient coupled climate model. *Climatic Change*, 43(2), 353-367.

Rahmstorf, S. (2002). Ocean circulation and climate during the past 120,000 years. *Nature*, 419(6903), 207-214.

Raymo, M. E. The initiation of Northern Hemisphere glaciation. *Annu. Rev. Earth Planet. Sci.* 22, 353–383 (1994).

Reid, J. L. (1978). On the middepth circulation and salinity field in the North Atlantic Ocean. *Journal of Geophysical Research: Oceans* (1978–2012), 83(C10), 5063-5067.

Reid, J. L. (1979). On the contribution of the Mediterranean Sea outflow to the Norwegian-Greenland Sea. *Deep Sea Research Part A. Oceanographic Research Papers*, 26(11), 1199-1223.

Rogerson, M., Rohling, E. J., Weaver, P. P. E., & Murray, J. W. (2005). Glacial to interglacial changes in the settling depth of the Mediterranean Outflow plume. *Paleoceanography*, 20(3).

Rogerson, M., Rohling, E. J., & Weaver, P. P. (2006). Promotion of meridional overturning by Mediterranean-derived salt during the last deglaciation. *Paleoceanography*, 21(4).

Rogerson, M., Colmenero-Hidalgo, E., Levine, R. C., Rohling, E. J., Voelker, A. H. L., Bigg, G. R., ... & Garrick, K. (2010). Enhanced Mediterranean-Atlantic exchange during Atlantic freshening phases. *Geochemistry, Geophysics, Geosystems*, 11(8).

Rogerson, M., Bigg, G. R., Rohling, E. J., & Ramirez, J. (2012). Vertical density gradient in the eastern North Atlantic during the last 30,000 years. *Climate dynamics*, 39(3-4), 589-598.

Rohling, E. J. (1994). Review and new aspects concerning the formation of eastern Mediterranean sapropels. *Marine Geology*, 122(1), 1-28.

Rosenthal, Y., and Wright, J. D. (2010). Traditional and emerging geochemical proxies in foraminifera. *The Journal of Foraminiferal Research*, 40(2), 165-192.

Ruddiman, W. F., & McIntyre, A. (1981). Oceanic mechanisms for amplification of the 23,000-year ice-volume cycle. *Science*, 212(4495), 617-627.

Schaeffer, M., Selten, F. M., Opsteegh, J. D., & Goosse, H. (2002). Intrinsic limits to predictability of abrupt regional climate change in IPCC SRES scenarios. *Geophysical Research Letters*, 29(16), 14-1.

Sachs, J. P., & Lehman, S. J. (1999). Subtropical North Atlantic temperatures 60,000 to 30,000 years ago. *Science*, 286(5440), 756-759.



- Sarmiento, J., and C. Le Quéré (1996), Oceanic carbon dioxide uptake in a model of century-scale global warming, *Science*, 274, 1346 – 1350.
- Sarnthein, M., Winn, K., Jung, S. J., Duplessy, J. C., Labeyrie, L., Erlenkeuser, H., & Ganssen, G. (1994). Changes in east Atlantic deepwater circulation over the last 30,000 years: Eight time slice reconstructions. *Paleoceanography*, 9(2), 209-267.
- Sarnthein, M., Stattegger, K., Dreger, D., Erlenkeuser, H., Grootes, P., Haupt, B. J., ... & Weinelt, M. (2001). Fundamental modes and abrupt changes in North Atlantic circulation and climate over the last 60 ky—Concepts, reconstruction and numerical modeling. In *The Northern North Atlantic* (pp. 365-410). Springer Berlin Heidelberg.
- Schmidt, M. W., Spero, H. J., and Lea, D. W. (2004). Links between salinity variation in the Caribbean and North Atlantic thermohaline circulation. *Nature*, 428(6979), 160-163.
- Schmittner, A., Latif, M., & Schneider, B. (2005). Model projections of the North Atlantic thermohaline circulation for the 21st century assessed by observations. *Geophysical Research Letters*, 32(23).
- Schmittner, A., Brook, E. J., & Ahn, J. (2007). Impact of the ocean's overturning circulation on Atmospheric CO<sub>2</sub>. *Ocean Circulation: Mechanisms and Impacts—Past and Future Changes of Meridional Overturning*, 315-334.
- Schönfeld, J. (2002). Recent benthic foraminiferal assemblages in deep high-energy environments from the Gulf of Cadiz (Spain). *Marine Micropaleontology*, 44(3), 141-162.
- Sexton, P. F., Wilson, P. A., and Pearson, P. N. (2006). Microstructural and geochemical perspectives on planktic foraminiferal preservation: “Glassy” versus “Frosty”. *Geochemistry, Geophysics, Geosystems*, 7(12).
- Sigman, D. M., & Boyle, E. A. (2000). Glacial/interglacial variations in atmospheric carbon dioxide. *Nature*, 407(6806), 859-869.
- Slangen, A. B. A., Katsman, C. A., van de Wal, R. S. W., Vermeersen, L. L. A., & Riva, R. E. M. (2012). Towards regional projections of twenty-first century sea-level change based on IPCC SRES scenarios. *Climate dynamics*, 38(5-6), 1191-1209.
- Spall, M. A., & Pickart, R. S. (2001). Where Does Dense Water Sink? A Subpolar Gyre Example\*. *Journal of Physical Oceanography*, 31(10), 2341-2347.
- Spall, M. A. (2010). Dynamics of downwelling in an eddy-resolving convective basin. *Journal of Physical Oceanography*, 40(10), 2341-2347.
- Spero, H. J., and Lea, D. W. (1993). Intraspecific stable isotope variability in the planktic foraminifera *Globigerinoides sacculifer*: Results from laboratory experiments. *Marine Micropaleontology*, 22(3), 221-234.
- Stanev, E. V. (1992). Numerical experiment on the spreading of Mediterranean water in the North Atlantic. *Deep Sea Research Part A. Oceanographic Research Papers*, 39(10), 1747-1766.
- Stocker, T. (1998) The seesaw effect. *Science* 282:61–62
- Stow, D.A.V., Hernández-Molina, F.J., Alvarez Zarikian, C.A., and the Expedition 339 Scientists Proceedings of the Integrated Ocean Drilling Program, Volume 339, 2013
- Timmermann, A., An, S. I., Krebs, U., & Goosse, H. (2005). ENSO suppression due to weakening of the North Atlantic thermohaline circulation. *Journal of Climate*, 18(16).
- Straneo, F. (2006). On the Connection between Dense Water Formation, Overturning, and Poleward Heat Transport in a Convective Basin\*. *Journal of physical oceanography*, 36(9), 1822-1840.
- Stuiver, M., Reimer, P. J., & Reimer, R. (2010). CALIB Rev. 6.0. 1 website program and documentation.
- Thiede, J., WINKLER, A., WOLF-WELLING, T. H. O. M. A. S., ELDHOLM, O., MYHRE, A. M., BAUMANN, K. H., ... & Stein, R. (1998). Late Cenozoic history of the polar North Atlantic: results from ocean drilling. *Quaternary Science Reviews*, 17(1), 185-208.
- Tomczak, M., & Godfrey, J. S. (2003). *Regional oceanography: an introduction*. Daya Books.
- Trenberth, K., Caron, J. (2001) Estimates of meridional atmosphere and ocean heat transport. *Clim. Dyn.* 14:3433–3443
- Våge, K., Pickart, R. S., Spall, M. A., Moore, G. W. K., Valdimarsson, H., Torres, D. J., ... & Nilsen, J. E. Ø. (2013). Revised circulation scheme north of the Denmark Strait. *Deep Sea Research Part I: Oceanographic Research Papers*, 79, 20-39. *Oceanography*, 31(3), 810-826.
- Vellinga, M., Wood, R. (2002) Global climatic impacts of a collapse of the Atlantic thermohaline circulation. *Clim Change* 54:251–267
- Voelker, A. H., Lebreiro, S. M., Schönfeld, J., Cacho, I., Erlenkeuser, H., & Abrantes, F. (2006). Mediterranean outflow strengthening during northern hemisphere coolings: a salt source for the glacial Atlantic?. *Earth and Planetary Science Letters*, 245(1), 39-55.
- Waelbroeck, C., Labeyrie, L., Michel, E., Duplessy, J. C., McManus, J. F., Lambeck, K., ... and Labracherie, M. (2002). Sea-level and deep water temperature changes derived from benthic foraminifera isotopic records. *Quaternary Science Reviews*, 21(1), 295-305.
- Weaver, A. J., and Hillaire-Marcel, C. (2004). Global warming and the next ice age. *Science (Washington)*, 304(5669), 400-402.
- Winton, M. (2003) On the climatic impact of ocean circulation. *J. Climate* 16:2875–2889
- Wolf-Welling, T. C. W., Thiede, J., & Myhre, A. M. Leg 151 Shipboard scientific party. 1995. Bulk sediment parameter and coarse fraction analysis: Paleoceanographic implications of Fram Strait Sites 908 and 909, ODP Leg 151 (NAAG). *Eos Transactions*, 76, 17.
- Wood, R. A., Keen, A. B., Mitchell, J. F., & Gregory, J. M. (1999). Changing spatial structure of the thermohaline circulation in response to atmospheric CO<sub>2</sub> forcing in a climate model. *Nature*, 399(6736), 572-575.
- Zickfeld, K., Levermann, A., Morgan, M. G., Kuhlbrodt, T., Rahmstorf, S., and Keith, D. W. (2007). Expert judgements on the response of the Atlantic meridional overturning circulation to climate change. *Climatic Change*, 82(3-4), 235-265.
- Zickfeld, K., Eby, M., & Weaver, A. J. (2008). Carbon-cycle feedbacks of changes in the Atlantic meridional overturning circulation under future atmospheric CO<sub>2</sub>. *Global Biogeochemical Cycles*, 22(3).